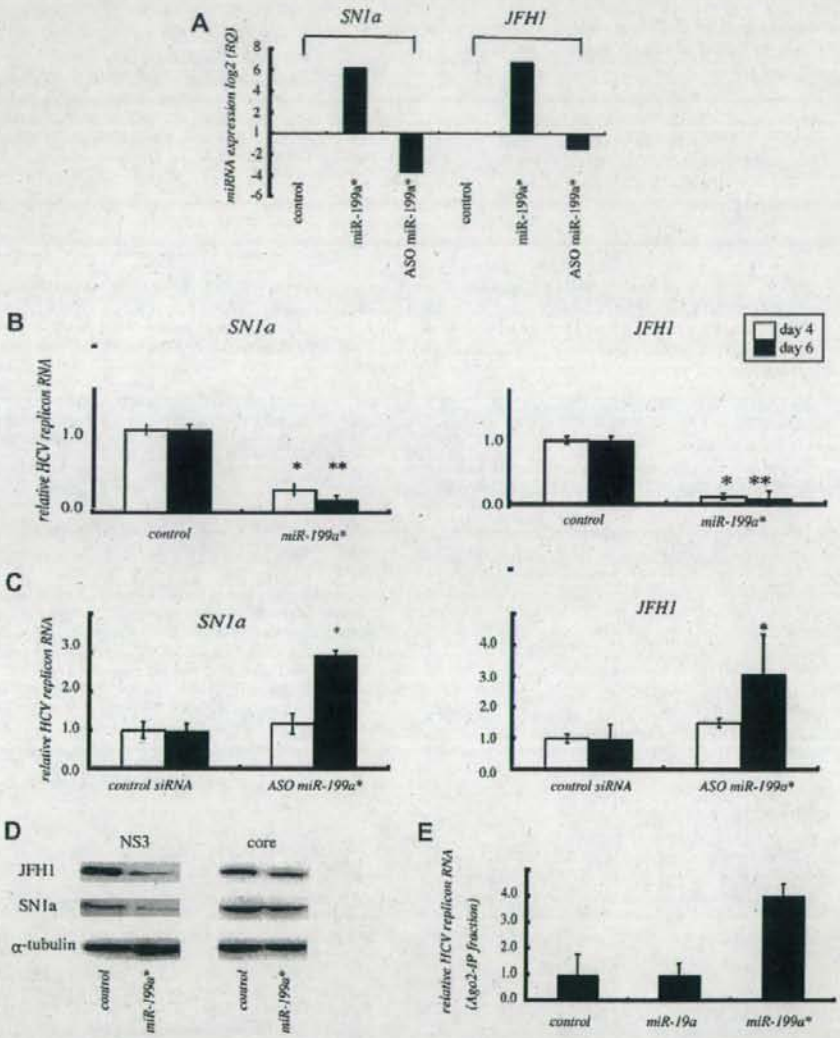

Fig. 2. Overexpression of miR-199a* decreased HCV replicon RNA levels. (A) Expression levels in SN1a and JFH1 cells after inducing overexpression of miR-199a* by miR-199a* expression vector or suppression of expression of miR-199a* by specific ASO were measured by real-time qPCR. (B) Comparison between HCV replicon RNA levels in SN1a (left) and JFH1 cell (right) before and after miRNA expression. The relative amounts of HCV replicon RNA per 50 ng of total RNA were measured by real-time qPCR at 4 and 6 days after transfection of miR-199a* and control vector. The data were normalized by the respective RNA levels in the controls. The data shown are as means ± SD of four independent experiments. *,Significant differences from the control at $p < 0.05$ and $p < 0.01$, respectively. (C) ASO with complementarity to miR-199a* stimulated HCV replicon RNA replication (left: SN1a cells, right: JFH1 cells). Relative amounts of HCV replicon RNA per 50 ng of total RNA were measured at day 4 and 6. (D) Immunoblot analysis of HCV core, NS3, and α-tubulin (internal control) in whole cell lysates from SN1a and JFH1 cells treated with miR-199a* expression or control vector. Fifty micrograms of whole cell lysates harvested 6 days after transfection was analyzed. (E) HCV replicon RNA is accumulated in RISC after miR-199a* expression. HCV replicon RNA was measured by real-time qPCR in 50 ng sample of total RNA from the Ago2-immunoprecipitation fraction.**

ViTa algorithms [22]. miR-199a* was identified as having a target sequence in the internal ribosomal entry site (IRES) of both the genotype 1b replicon (Con 1; GeneBank Accession No. AJ238799) and 2a (JFH1; GeneBank Accession No. AB047639) (Fig. 1). Endogenous expression levels of miR-199a* and 122 in Hela, Huh-7, SN1a (containing Con 1 replicon (genotype 1b)) cells, and normal liver tissue were shown (Supplementary

Fig. 1). Endogenous expression level of miR-122 was abundant in Huh-7, SN1a, and normal liver tissue [6] and endogenous expression level of miR-199a* in Huh-7 and SN1a was more than in normal liver tissue.

3.2. miR-199a* overexpression suppresses the replication of HCV replicon

This study showed that the expression level of miR-199a* was modified by the expression vector and by ASO complementary to miR-199a* in cells bearing either replicon, SN1a or JFH1 (Fig. 2A). Overexpression markedly restricted replicon replication in both cell lines (Fig. 2B). To determine whether miR-199a* has specific anti-viral effects, we inhibited miR-199a* activity with ASO. HCV replicon replication significantly increased in both cell lines upon treatment with ASO on day 4 and 6 (Fig. 2C). Immunoblot analysis showed good concordance with the result of real-time qPCR (Fig. 2D).

3.3. Ago2 co-immunoprecipitates target mRNA

To show that miR-199a* is associated with HCV genome physiologically [23], we performed an Ago2-co-immunoprecipitation (Ago2-IP) analysis to see whether

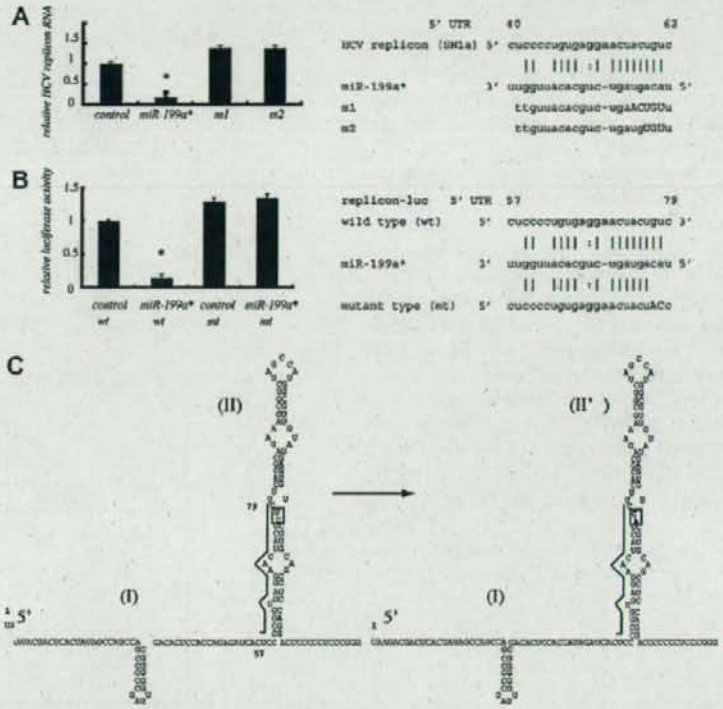

Fig. 3. Suppression of HCV replicon activity by miR-199a* was abolished by mutations in either the miRNA sequence or the miR-199a* target sequence in the HCV-replicon-luciferase construct. (A) Effect of mutated miR-199a* on HCV replicon activity. Comparison of HCV replicon RNA level in SN1a expressing ectopically with wild-type and mutated miRNAs measured by real-time qPCR. Complementarity among HCV replicon genome (upper number corresponds to the 5′-UTR start codon) and miR-199a* and two types of mutated miR-199a*: m1 and m2 are shown. Mutated nucleotides in m1 and m2 sequences are shown in capital letters. Additional nucleotides added to stabilize m1 and m2 are represented by tt. Relative HCV replicon RNA levels were normalized to the control siRNA level and are expressed as means ± SD of four independent experiments. *Significant difference at $p < 0.05$. (B) Effect of the miR-199a* on the wild-type and mutant-type HCV replicon activities. Comparison between the level of replicon activity in cured MH14 cell lysate after co-transfected of either miR-199a* expression vector or control vector, and either wild-type or mutant-type HCV replicon-luciferase construct. Sequences of wild-type (upper) and mutant-type (lower) HCV-replicon-luciferase in the IRES region are shown. Vertical bars and horizontal bars indicate complementary bases and gaps in complementarity between miR-199a* and the HCV-replicon-luciferase [13]. Mutated nucleotides are shown in capital letters. Nucleotide numbers begin at the start codon in the IRES. Mutated HCV-replicon-luciferase (mt) reduced the inhibitory effect of miR-199a*. Each column represents luciferase values standardized to the control vector co-transfected with the wild-type HCV-replicon-luciferase. The data shown are means ± SD of three replicates. (C) The target region of miR-199a* in the stem-loop II in IRES and the upstream stem-loop I together with its flanking region is shown. Small numbers indicate nucleotide positions from the 5′ end [28]. The thick bar indicates the target site. The mutated sequence is shown in II′ with the mutated residues boxed.

RISC could retain HCV genome when miR-199a* was over-produced. SN1a cells were transfected with either miR-199a*, miR-19a expression vector, or a control vector and used to prepare respective Ago2-IP fractionated cell lysates. Since miR-19a* does not recognize either HCV genome 1b or 2a, we used miR-19a as a negative control. The HCV-replicon RNA in the Ago2-IP fraction (IP RNA) was quantified by real-time qPCR. The concentration of HCV-replicon RNA was higher in the IP-RNA obtained by treatment with miR-199a* than by treatment with the control expression vector or miR-19a expression vector (Fig. 2E).

3.4. Effects of mutated miRNA sequences and target site sequences on miRNA suppression

We synthesized two miRNAs, with 5 and 3 bases in the sequence of mutated miR-199a*, yielding m1, and m2. We chose the mutation sites shown in Fig. 3. Transfection of m1 and m2 into SN1a cell did not suppress HCV RNA levels (Fig. 3A).

Mutated HCV-replicon-luciferase construct with two point mutations in the putative binding site of targeted by miR-199a* in the IRES region was synthesized. The luciferase activity of the wild-type replicon on IRES region decreased with treatment of miR-199a* expression vector as compared control expression vector. However, the luciferase activity of the replicon-luciferase with a mutated sequence in the IRES was unaltered by treatment with either miR-199a* or control expression vector (Fig. 3B). Since the recognition site is located in the stem-loop II in the IRES, the mutation was introduced so that the secondary structure of the stem-loop II would be unchanged. Although we did not verify the secondary structure of the mutated stem-loop II by biochemical analysis, "RNA secondary structure prediction" software (http://www.genebee.msu.su/services/rna2_reduced.html) predicted it to be the original structure (Fig. 3C).

3.5. Pretreating immortalized hepatocytes with miRNA reduces HCV replication

Immortalized HuS-E/2 cells ectopically expressing miR-199a* were infected with serum from an HCV-1b or HCV-2a-infected patients. The HCV replication was significantly lower in cells expressing miR-199a*, irrespective of the HCV genotype (Fig. 4A). In contrast, treatment of the cells before HCV infection with miR-199a* ASO caused to accumulate HCV RNA (Fig. 4B). We then performed an *in vitro* infection study with the infectious recombinant HCV-JFH1 virus. HuS-E/2 cells were inoculated with concentrated JFH1 medium. In HuS-E/2 cells after treatment with miR-199a* ASO, we found an increase in JFH1-RNA (Fig. 4C).

3.6. The anti-viral effect of miR-199a is independent of the interferon (IFN) pathway*

Cured MH14, HepG2, and Huh-7 cells co-transfected with the ISRE-luciferase reporter and either miR-199a* expression vector or the control vector were harvested and analyzed for luciferase activity. There was no significant difference in luciferase activity between the control and the miR-199a*-treated group (Fig. 5A) [24]. Moreover, no expression of the IFN-induced genes; MxA, PKR, and 2′-5′-OAS was induced by treatment of miR-199a* (Fig. 5B).

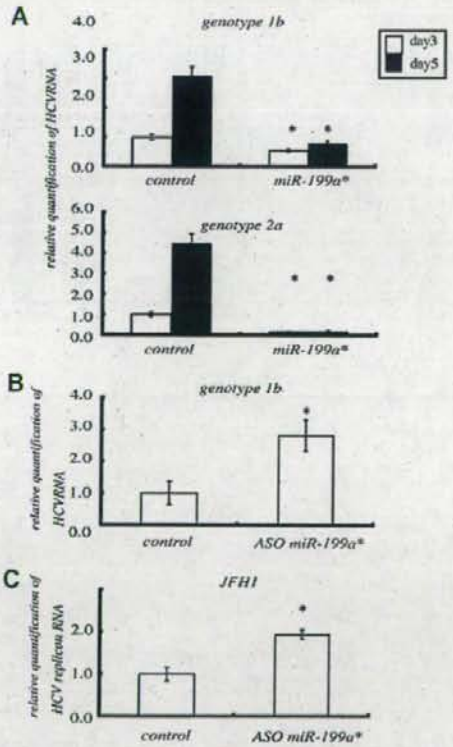

Fig. 4. Overexpression of miR-199a* reduced HCV replication. (A) Overexpression of miR-199a* reduced the amount of HCV RNA in HuS-E/2 cells infected with serum containing HCV-genotype 1b and 2a, in comparison with the control vector. Each column represents the relative amount of HCV RNA normalized to the vector control sample on post-transfection day 3 and 5. The data shown are means ± SD of four independent experiments. *,Significant difference at $p < 0.05$ and $p < 0.01$, respectively. (B) Prior transfection of HuS-E/2 cells with miR-199a* ASO accelerated HCV-1b replication activity on day 3. HCV RNA levels are expressed as means ± SD of four independent experiments. (C) miR-199a* ASO prior to *in vitro* infection with JFH1 replicon RNA accelerated JFH1 replicon RNA. Experimental procedure is described in Section 2.**

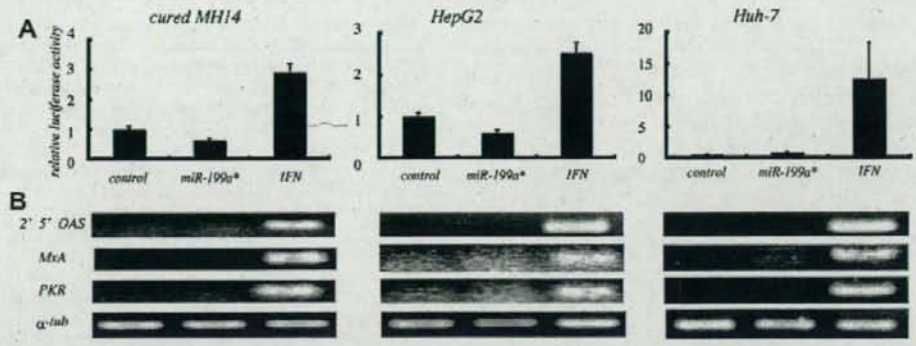

Fig. 5. Treatment of the cells with miR-199a* did not induce the IFN pathway. (A) Cured MH14 (left), HepG2 (middle) and Huh-7 cells (right) were co-transfected with pISRE-Luc and either miR-199a* expression vector or the control vector. In a control experiment to investigate IFN response, one line of cells treated with IFNα (500 IU/ml) for 6 h at 90 h after transfection of the control vector. The cellular luciferase activity was measured 96 h after transfection and normalized to luciferase activity of the cells treated with the control vector treatment. Each column represents the luciferase activity, normalized to the control vector. (B) 2′-5′-OAS, MxA, and PKR expression was measured by semi-quantitative RT-PCR on day 4 after transfection.

4. Discussion

This study demonstrates that HCV replication can be controlled by miRNA. Viruses use non-coding RNAs, such as miRNAs, to inhibit intrinsic anti-viral immunity in mammalian cells. For example, herpesvirus encodes viral miRNAs that dampen host antiviral immunity [25], and many mammalian viruses usurp or divert host mRNA silencing machinery to their advantage. By contrast, some host-encoded miRNAs have anti-viral functions [26]. RNA silencing-based antiviral responses may work in concert with innate and acquired antiviral systems [27].

miR-199a* has a target sequence in domain II of the IRES region in the HCV 5′-UTR, a region that is highly conserved across all HCV genotypes [28] and is crucial for viral replication. Introduction of miR-199a* ASO into replicon cells had the opposite effect of increasing viral replication. Mutagenesis analyses showed that the inhibitory effect of miR-199a* on HCV replication was highly dependent on complementarity between the viral and host sequences. Because HCV-replicon RNA is concentrated in the RISC by overexpression of miR-199a*, miR-199a* and HCV-replicon RNA seem be complexed in cells under certain pathophysiological conditions. Our study indicates that the sequence-dependent interactions contribute to the anti-HCV activities of miR-199a*.

However, miRNAs often recognize target genes with incomplete complementarity, which allows them to recognize many target-candidate genes. To determine whether the anti-viral effect of the miRNA is mediated not only by mechanism that directly targets the HCV genome but by other mechanism, such as modulation of cellular genes, we analyzed the mRNA expression profiles of miR-199a*-transfected cells by microarray. Based on the results of the microarray analysis, as shown in Supplementary Fig. 2, we identified several genes whose expression level changed at least twofold after overexpression. Ceruloplasmin (CP) has already been reported to be involved in HCV replication [29]. Although CP is not contained in a list of miRase targets (http://microrna.sanger.ac.uk/target/v5/) for miR-199a*, it will be necessary to determine whether CP is controlled by miR-199a* as miRNA machinery and whether CP is capable of participating in HCV replication.

Chronic HCV infection causes various liver diseases, from chronic hepatitis to hepatocellular carcinoma. Previously we demonstrated that miRNA expression profiles change with the degree of liver fibrosis and pathological differentiation of HCC [18]. In the present study we demonstrated that miR-199a* can control viral replication. miRNAs may have future application as efficient, safe, and specific means of antiviral therapy.

Acknowledgments

We thank R. Bartenschlager at Heidelberg University for providing the Con 1 strain and Kaku Goto for technical assistance. Y.M. and K.S. were supported by the Ministry of Health, Labour and Welfare of Japan; grants-in-aid for scientific research from the Ministry of Education, Culture, Sports, Science and Technology of Japan.

Appendix A. Supplementary data

Microarray analysis. Fluorescent (cyanine 3-CTP)-labeled cRNA was synthesized from 500 ng of total RNA with a Low RNA Input Fluorescent Linear

Amplification Kit (Agilent Technologies), and hybridized to a Human 1A(v2) Oligo microarray (Agilent Technologies). The signal intensity per spot was analyzed from scanned images using Feature Extraction Software ver8.5 (Agilent Technologies). To compare expression profiles between miRNA-transfected and control cells, median percentile normalization was performed using GeneSpring GX 7.3 (Agilent Technologies).

Supplementary data associated with this article can be found, in the online version, at doi:10.1016/j.jhep.2008.06.010.

References

[1] Wasley A, Alter MJ. Epidemiology of hepatitis C: geographic differences and temporal trends. Semin Liver Dis 2000;20:1–16.

[2] Foster GR. Past, present, and future hepatitis C treatments. Semin Liver Dis 2004;24:97–104.

[3] McHutchison JG, Gordon SC, Schiff ER, Shiffman ML, Lee WM, Rustgi VK, et al. Interferon alfa-2b alone or in combination with ribavirin as initial treatment for chronic hepatitis C. Hepatitis Interventional Therapy Group. New Engl J Med 1998;339:1485–1492.

[4] Pillai RS. MicroRNA function: multiple mechanisms for a tiny RNA? RNA 2005;11:1753–1761.

[5] Zamore PD, Haley B. Ribo-gnome: the big world of small RNAs. Science 2005;309:1519–1524.

[6] Lagos-Quintana M, Rauhut R, Yalcin A, Meyer J, Lendeckel W, Tuschl T. Identification of tissue-specific microRNAs from mouse. Curr Biol 2002;12:735–739.

[7] Jopling CL, Yi M, Lancaster AM, Lemon SM, Sarnow P. Modulation of hepatitis C virus RNA abundance by a liver-specific MicroRNA. Science 2005;309:1577–1581.

[8] Randall G, Panis M, Cooper JD, Tellinghuisen TL, Sukhodolets KE, Pfeffer S, et al. Cellular cofactors affecting hepatitis C virus infection and replication. Proc Natl Acad Sci USA 2007;104:12884–12889.

[9] Henry SD, van der Wegen P, Metselaar HJ, Tilanus HW, Scholte BJ, van der Laan LJ. Simultaneous targeting of HCV replication and viral binding with a single lentiviral vector containing multiple RNA interference expression cassettes. Mol Ther 2006;14:485–493.

[10] Kapadia SB, Brideau-Andersen A, Chisari FV. Interference of hepatitis C virus RNA replication by short interfering RNAs. Proc Natl Acad Sci USA 2003;100:2014–2018.

[11] Wang Y, Kato N, Jazag A, Dharel N, Otsuka M, Taniguchi H, et al. Hepatitis C virus core protein is a potent inhibitor of RNA silencing-based antiviral response. Gastroenterology 2006;130:883–892.

[12] Yokota T, Sakamoto N, Enomoto N, Tanabe Y, Miyagishi M, Maekawa S, et al. Inhibition of intracellular hepatitis C virus replication by synthetic and vector-derived small interfering RNAs. EMBO Rep 2003;4:602–608.

[13] Murata T, Ohshima T, Yamaji M, Hosaka M, Miyanari Y, Hijikata M, et al. Suppression of hepatitis C virus replicon by TGF-beta. Virology 2005;33:407–417.

[14] Ishii N, Watashi K, Hishiki T, Goto K, Inoue D, Hijikata M, et al. Diverse effects of cyclosporine on hepatitis C virus strain replication. J Virol 2006;80:4510–4520.

[15] Wakita T, Pietschmann T, Kato T, Date T, Miyamoto M, Zhao Z, et al. Production of infectious hepatitis C virus in tissue culture from a cloned viral genome. Nat Med 2005;11:791–796.

[16] Aly HH, Watashi K, Hijikata M, Kaneko H, Takada Y, Egawa H, et al. Serum-derived hepatitis C virus infectivity in interferon regulatory factor-7-suppressed human primary hepatocytes. J Hepatol 2007;46:26–36.

[17] Watashi K, Hijikata M, Hosaka M, Yamaji M, Shimotohno K. Cyclosporin A suppresses replication of hepatitis C virus genome in cultured hepatocytes. Hepatology 2003;38:1282–1288.

[18] Murakami Y, Yasuda T, Saigo K, Urashima T, Toyoda H, Okanoue T, et al. Comprehensive analysis of microRNA expression patterns in hepatocellular carcinoma and non-tumorous tissues. Oncogene 2006;25:2537–2545.

[19] Kato N, Ikeda M, Mizutani T, Sugiyama K, Noguchi M, Hirohashi S, et al. Replication of hepatitis C virus in cultured non-neoplastic human hepatocytes. Jpn J Cancer Res 1996;87:787–792.

[20] Ohshima T, Shimotohno K. Transforming growth factor-beta-mediated signaling via the p38 MAP kinase pathway activates Smad-dependent transcription through SUMO-1 modification of Smad4. J Biol Chem 2003;278:50833–50842.

[21] MacQuillan GC, Mamotte C, Reed WD, Jeffrey GP, Allan JE. Upregulation of endogenous intrahepatic interferon stimulated genes during chronic hepatitis C virus infection. J Med Virol 2003;70:219–227.

[22] Hsu PW, Lin LZ, Hsu SD, Hsu JB, Huang HD. ViTa: prediction of host microRNAs targets on viruses. Nucleic Acids Res 2007;35:D381–D385.

[23] Karginov FV, Conaco C, Xuan Z, Schmidt BH, Parker JS, Mandel G, et al. A biochemical approach to identifying microRNA targets. Proc Natl Acad Sci USA 2007;104:19291–19296.

[24] Naganuma A, Nozaki A, Tanaka T, Sugiyama K, Takagi H, Mori M, et al. Activation of the interferon-inducible 2′-5′-oligoadenylate synthetase gene by hepatitis C virus core protein. J Virol 2000;74:8744–8750.

[25] Umbach JL, Kramer MF, Jurak I, Karnowski HW, Coen DM, Cullen BR. MicroRNAs expressed by herpes simplex virus 1 during latent infection regulate viral mRNAs. Nature 2008;454:780–783.

[26] Cullen BR. Viruses and microRNAs. Nat Genet 2006;38:S25–S30.

[27] Rehermann B, Nascimbeni M. Immunology of hepatitis B virus and hepatitis C virus infection. Nat Rev 2005;5:215–229.

[28] Houda A, Arai Y, Hirota N, Sato T, Ikegaki J, Koizumi T, et al. Hepatitis C virus structural proteins induce liver cell injury in transgenic mice. J Med Virol 1999;59:281–289.

[29] Fillebeen C, Muckenthaler M, Andriopoulos B, Bisaillon M, Mounir Z, Hentze MW, et al. Expression of the subgenomic hepatitis C virus replicon alters iron homeostasis in Huh7 cells. J Hepatol 2007;47:12–22.

Biochemical and Biophysical Research Communications 379 (2009) 330-334

Contents lists available at ScienceDirect

Biochemical and Biophysical Research Communications

journal homepage: www.elsevier.com/locate/ybbrc

3D cultured immortalized human hepatocytes useful to develop drugs for blood-borne HCV

Hussein Hassan Aly [a], Kunitada Shimotohno [b], Makoto Hijikata [a,c,*]

[a] Laboratory of Human Tumor Viruses, The Institute for Virus Research, Kyoto University, Department of Viral Oncology, 53 Kawaharacho, Shogoin, Sakyoku, Kyoto 606-8507, Japan
[b] Center for Human Metabolomic Systems Biology, Keio University, 35 Shinano-machi, Shinjuku-ku, Tokyo 160-8582, Japan
[c] Laboratory of Viral Oncology, Graduate School of Biostudies, Kyoto University, Konoecho, Yoshida, Sakyoku, Kyoto 606-8501, Japan

ARTICLE INFO

Article history:
Received 5 December 2008
Available online 25 December 2008

Keywords:
Hepatitis C virus
Infection
Replication
3D culture
PPAR
Immortalized hepatocytes
Blood-borne HCV

ABSTRACT

Due to the high polymorphism of natural hepatitis C virus (HCV) variants, existing recombinant HCV replication models have failed to be effective in developing effective anti-HCV agents. In the current study, we describe an *in vitro* system that supports the infection and replication of natural HCV from patient blood using an immortalized primary human hepatocyte cell line cultured in a three-dimensional (3D) culture system. Comparison of the gene expression profile of cells cultured in the 3D system to those cultured in the existing 2D system demonstrated an up-regulation of several genes activated by peroxisome proliferator-activated receptor alpha (PPARα) signaling. Furthermore, using PPARα agonists and antagonists, we also analyzed the effect of PPARα signaling on the modulation of HCV replication using this system. The 3D *in vitro* system described in this study provides significant insight into the search for novel anti-HCV strategies that are specific to various strains of HCV.

Infection with Hepatitis C virus (HCV) is a serious health problem worldwide and leads to high rates of liver cirrhosis and hepatocellular carcinoma [1]. Given that the standard HCV therapy remains insufficient for the successful treatment of many patients [2], the development of more effective and less toxic anti-HCV agents is required. *In vitro* systems like the HCV replicon-bearing cells and the infectious particle-producing JFH1 system, has contributed to the discovery of new targets for anti-HCV therapy. However, these recombinant HCV genomes only proliferate in sublines of HuH-7 cells, which do not permit infection or proliferation of blood-borne HCV. Due to the high polymorphism of natural HCV, data from recombinant HCV systems could be evaluated by studying the therapeutic response of a variety of naturally occurring HCVs. However, the current systems available for such study remain insufficient due to the low infection and replication efficiency of the natural HCV strains.

More recently, production and secretion of infectious HCV particles has been reported in two independent three-dimensional (3D) cell culture systems, termed the radial-flow bioreactor (3D/RFB) and the thermoreversible gelatin polymer (3D/TGP) systems. These results were not observed in monolayer cultures [3], suggesting that hepatocytes cultured in 3D more closely resemble liver cells *in vivo* [4] and thus support HCV proliferation. In addition, analysis of gene expression levels in 3D cultured cells revealed that the newly established immortalized human hepatocyte (HuS-E/2 cells) gene profile was altered to more closely resemble that of human liver tissue when the cells were cultured in 3D/TGP [5].

In the current study, we cultured HuS-E/2 cells in 3D/TGP and demonstrated efficient proliferation of natural HCV. Furthermore, gene expression analysis of these cells demonstrated the activation of the peroxisome proliferators-activated receptor α (PPARα) signaling pathway, suggesting an important role for this pathway in the replication of natural HCV. Thus, the *in vitro* system described appears to be a useful tool for the study of HCV infection and proliferation as well as for the development of effective anti-viral agents against various natural HCVs.

Materials and methods

Cell culture. Immortalized human hepatocytes (HuS-E/2) and LucNeo#2 replicon cells [6] were cultured as previously described [5,7]. For the 3D-TGP culture system, 1×10^5 HuS-E/2 cells were cultured in 1 ml Mebiol gel (Mebiol Inc., Kanagawa, Japan)/well in 12-well plates. Five hundred microliters of fresh medium was overlaid on the solidified gel, and was changed every 2 days. Cell

* Corresponding author. Address: Laboratory of Human Tumor Viruses, The Institute for Virus, Kyoto University, Department of Viral Oncology, 53 Kawaharacho, Shogoin, Sakyoku, Kyoto 606-8507, Japan. Fax: +81 75 751 3998.
E-mail address: mhijikat@virus.kyoto-u.ac.jp (M. Hijikata).

0006-291X/$ - see front matter © 2008 Elsevier Inc. All rights reserved.
doi:10.1016/j.bbrc.2008.12.054

extraction from the gel was done at the designated time points according to the manufacturer's protocol.

RNA extraction, reverse transcriptase polymerase chain reaction (RT-PCR) and real-time RT-PCR (Q-PCR). At the designated time points, total cellular RNA was extracted and 1 μg of total RNA was used as a template for RT-PCR and for the quantitative detection of HCV-RNA using real-time RT-PCR (Q-PCR) as previously described [10].

HCV infection experiment. HCV infection experiments were carried out using sera from patients infected with HCV. Infection in 2D culture was undertaken as previously described [5]. For 3D/TGP cultured cells, the gel was solidified, and 50 μl HCV-containing patient serum with a titer of 1×10^6 HCV-RNA/ml was added to the culture and mixed. The culture was continued until the cells were extracted. Following extraction from 3D-TGP, cells were centrifuged and washed three times thoroughly with PBS. RNA was then extracted from the cells as described above. HCV infection into HuS-E/2 cells was also examined in the presence of anti-E2 mouse monoclonal antibody (917) as outlined previously [8].

Treatment of cells with PPARα signaling agonists and antagonists. Fenofibrate or MK886 (Sigma–Aldrich, USA) were added to the culture medium of HuS-E/2 (2D-HuS-E/2) cells from day 0 of HCV infection; or the culture medium of LucNeo#2 replicon harboring cells. The cells were then cultured to the designated time point.

Microarray analysis. Gene expression profiles of 3D/TGP cultured HuS-E/2 cells were obtained by microarray analysis (3D-Genes Human 25, Toray, Tokyo, Japan) and compared to those of cells cultured in 2D.

Results

3D/TGP cultures enhance HCV proliferation in HuS-E/2 cells

Infection and proliferation of the HCV genotype 1b (HCV-RC5) derived from the serum of patient RC5 in HuS-E/2 cells cultured in 3D/TGP (3D/TGP-HuS-E/2 cells) was investigated and compared with that of HuS-E/2 cells cultured in 2D (2D-Hus-E/2). As outlined in Fig. 1A, the HCV-RNA levels in the 3D/TGP-HuS-E/2 cells were significantly higher at all of the time points examined following infection than in the 2D-HuS/E2 cells, suggesting that the 3D/TGP system greatly enhances the proliferation of naturally occurring HCV in HuS-E/2 cells. Similar results were also obtained for sera from additional patients (data not shown). To examine whether the infection is viral envelope-receptor mediated, the infection experiments using serum treated with anti-HCV-E2 antibody (α-E2) or with anti-tubulin (negative control) was also performed. Pre-incubation of the serum with α-E2 significantly reduced the total amount of HCV-RNA in the cells upon infection (Fig. 1B). This result suggested that the infection of natural HCV into 3D/TGP-HuS-E/2 cells was HCV-E2-dependent.

Inhibition of natural HCV replication in HuS-E/2 cells by Interferon

In order to test the effects of anti-viral agents on natural HCV replication in 3D/TGP HuS-E/2 cells, 50–100 U/ml of IFNα was added to the medium overlaying the HCV-RC5 infected 3D/TGP-HuS-E/2 cells. The two treatment concentrations resulted in the inhibition of HCV-RNA replication in 3D-HuS-E/2 cells by

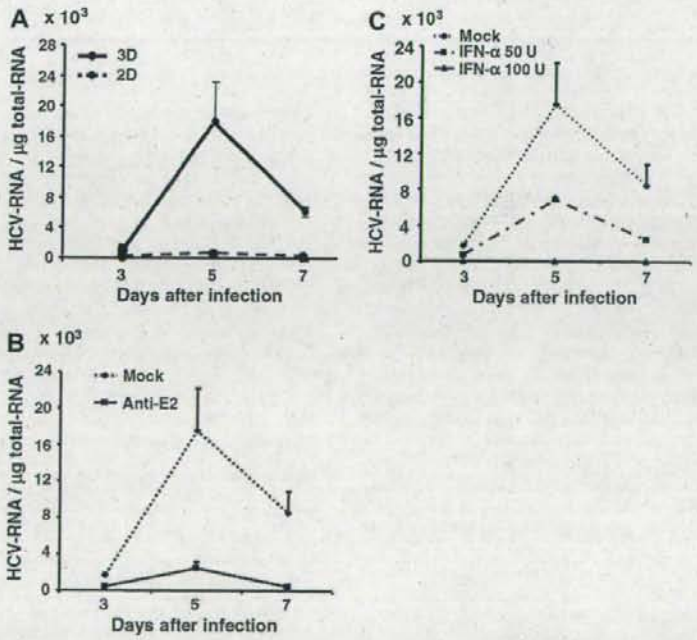

Fig. 1. HCV infection into 3D/TGP-HuS-E/2 cells. (A) 3D/TGP significantly enhanced HCV proliferation in HuS-E/2 cells. HCV patient serum was used to infect a similar number of HuS-E/2 cells cultured in 2D (hashed line) or 3D/TGP (solid line) culture for 24 h. Cells were then harvested and lysed at the indicated time points (3–7 days). The quantity of genomic HCV-RNA per 1 μg total RNA was determined by Q-PCR analysis. (B) Anti-E2 antibodies blocked HCV infection. HCV infection was performed as described in panel A in the presence of Anti-E2 specific or anti-tubulin (control) antibodies. (C) IFNα inhibits HCV replication in 3D/TGP-HuS-E/2 cells. HuS-E/2 cells were infected with HCV and fresh medium supplemented with or without (Mock), 50 U/ml, or 100 U/ml IFNα overlaid on the gel containing the cells and HCV proliferation measured as described above.

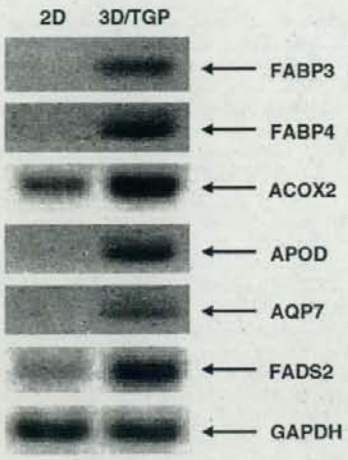

Fig. 2. RT-PCR analysis of the expression of genes identified by microarray. The PPARα regulated genes were increased in 3D/TGP-HuS-E/2 cells (3D-TGP) and their expression levels measured by RT-PCR. 2D represents RNA samples from 2D-HuS -E/2 cells. Twenty cycles of amplification were undertaken for the RT-PCR analysis. GAPDH expression served as an internal control. *Abbreviations:* FABP3, fatty acid binding proteins 3; FABP4, fatty acid binding proteins 4; ACOX2, acyl-coenzyme A oxidase 2; APOD, apolipoprotein D; AQP7, aquaporin 7; FADS2, fatty acid desaturase 2; GAPDH, glyceraldehyde 3-phosphate dehydrogenase.

approximately 50–60% and almost completely, respectively, when compared to the replication in cells receiving mock treatment (Fig. 1C). These results demonstrate that the IFNα treatment was effective on HCV derived from RC5 and that 3D/TGP-HuS-E/2 cells may be useful for the screening of anti-HCV drugs for the treatment of natural HCV.

Increased activation of the PPARα signaling pathway in 3D cultured HuS-E/2 cells

Given that 3D/TGP-HuS-E/2 cells demonstrated enhanced proliferation of natural HCV, the gene expression profiles of these cells was compared with that of cells cultured under normal 2D conditions using microarray analysis in order to identify the factors required for the enhanced proliferation. Among the 24,268 genes compared in this analysis, 212 genes demonstrated a greater than four folds index increase in expression in 3D/TGP than standard cultured cells. Cell signaling pathway analysis of these 212 genes showed that six genes, including fatty acid binding proteins 4 and 3 (FABP4 and 3), apolipoprotein D (APOD), aquaporin 7 (AQP7), acyl-coenzyme A oxidase 2 (ACOX2), and fatty acid desaturase 2 (FADS2), were targets of PPARα signaling [9–12]. The increased expression of these genes in the 3D/TGP-HuS-E/2 cells was further confirmed by RT-PCR analysis (Fig. 2). Given that PPARα is an essential factor for normal hepatocyte function [13], these results indicate that 3D/TGP culture enhances the hepatocyte-specific characteristics of HuS-E/2 cells.

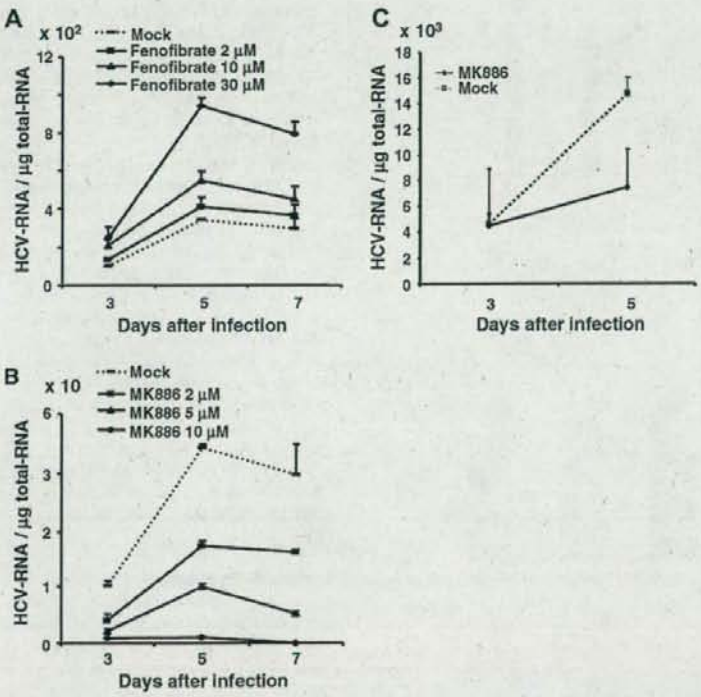

Fig. 3. The effects of PPARα agonists and antagonists on natural HCV proliferation. (A) HuS-E/2 cells were infected with HCV and fresh medium supplemented with or without (Mock) 2, 10, or 30 μM of fenofibrate overlaid on the cells. (B) Medium supplemented with or without (Mock), 2, 5, or 10 μM of MK886 was overlaid on 2D-HuS-E/2 cells infected with HCV. HCV proliferation following treatment was measured by Q-PCR. (C) Medium supplemented with or without (Mock), 10 μM of MK886 was overlaid on 3D/TGP-HuS-E/2 cells infected with HCV. HCV proliferation following treatment was measured by Q-PCR.

PPARα signaling affects HCV replication

We next examined the potential role of PPARα signaling on HCV proliferation by monitoring HCV replication in 2D-HuS-E/2 cells that had been infected with HCV-RC5 and subsequently treated with the PPARα agonist fenofibrate [14] or the PPARα antagonist MK886 [14] (Fig. 3B). As outlined in Fig. 3A, a dose-dependent increase in HCV replication was observed in fenofibrate-treated cells. In contrast, a dose-dependent decrease in HCV proliferation was observed in the presence of MK886. Similarly, treatment with MK886 reduced HCV proliferation in 3D/TGP-HuS-E/2 cells (Fig. 3C). The response of HCV proliferation in response to fenofibrate and MK886 treatment was also analyzed in LucNeo#2 cells that contained HCV replicon RNA (LNMH14) derived from the HCV-1b genome (Fig. 4A). Luciferase expression in these cells represented replication of the HCV replicon [6] and, as shown in Fig. 4A, luciferase activity in the cells treated with fenofibrate or MK886 also showed either enhancement or suppression of replicon proliferation, respectively. In addition, the increased HCV replication following fenofibrate treatment was completely abolished when treated with MK886 simultaneously. As MK886 is known to induce apoptosis when administered in high doses [15], the cell viability was examined using the XTT assay. There were no significant effects on cell viability after treatment with fenofibrate. Although MK886 resulted in a minor reduction in XTT values when high doses (10–15 μM) were administered, this reduction was not statistically significant when compared to its effect on HCV replication (Fig. 4B). This result suggests that PPARα signaling is required for HCV replication and that suppression of PPARα signaling has an anti-HCV effect.

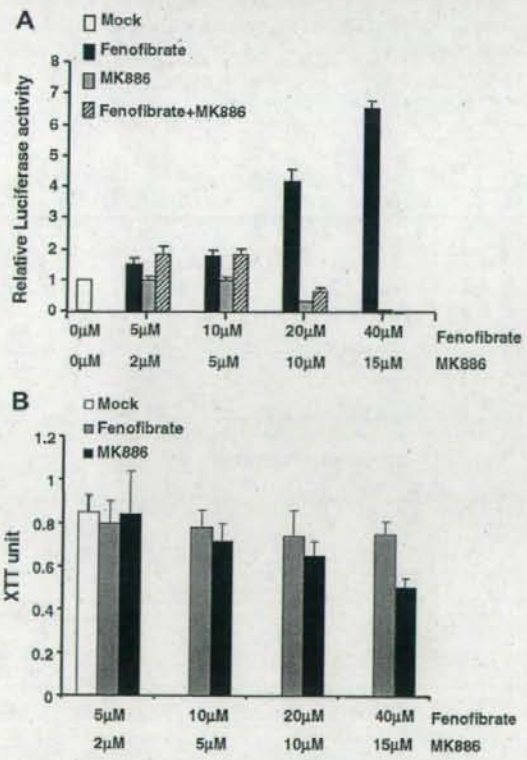

Fig. 4. The effects of PPARα agonists and antagonists on the replication of HCV subgenomic replicons. (A) LucNeo#2 cells containing a HCV subgenomic replicon termed LNMH14, were mock treated or treated with fenofibrate, MK886, or a combination of both fenofibrate and MK886 at the indicated concentrations for 2 days. Luciferase activity derived from the replicon was then measured as an indicator of HCV replication [7]. (B) Following treatment with fenofibrate and Mk886, LucNeo#2 cells were cultured for 2 days and cell viability measured using the XTT assay (Roche, Mannheim, Germany).

Discussion

In the current study, we demonstrated that immortalized hepatocyte HuS-E/2 cells cultured in 3D/TGP support the infection and replication of natural HCV derived from patient sera. Unlike recombinant HCVs, which have been required to adapt to sublines of HuH-7 cells [16], the population of the natural HCV is fairly polymorphic, demonstrating different responses to a variety of anti-viral agents [17,18]. The 3D/TGP-HuS-E/2 cells have the advantage of being a small-scale 3D cultured cells, which are cultured in 12-well plates at a density of 1×10^5/well, that allow the study of both viral and cellular events. In the current study, it demonstrated a 2 log increase in susceptibility to natural HCV infection and replication when compared to conventional 2D culture systems. Thus it offers an important advantage in the study of natural HCV infection and replication, and the response of natural HCV to anti-HCV drugs.

As the ability of HuS-E/2 cells to support infection and replication of natural HCV was greatly altered by the culture conditions, it is likely that the culture system described in our study will provide important information in regards to the cellular factors that support the HCV life cycle. The microarray study showed that the expression of some genes related to the PPARα signaling pathway were upregulated in the 3D cultured HuS-E/2 cells. Using both PPARα signaling agonists and antagonists, PPARα signaling was shown to affect infection and proliferation of natural HCV. PPARα is a ligand-activated transcription factor that is primarily expressed in tissues with high lipid metabolism including the liver, where it functions as one of three major nuclear receptors and is essential for its normal function [19]. Similar to a part of our data, a negative effect on HCV replication was previously observed in the replicon-bearing cells treated with siRNA for PPARα, with only 50% reduction of HCV-RNA [20]. In this study, even a large dose of PPARα agonist enhanced natural HCV replication in the 2D-HuS-E/2 cells for three times, despite the 2 logs enhancement of HCV proliferation in 3D/TGP culture. This implies that additional factors activated in 3D/TGP-HuS-E/2 cells may be required for the efficient HCV proliferation. Further analysis of the microarray data may provide us with further information on factors that may prove useful in the development of anti-HCV drugs.

In conclusion, the novel *in vitro* culture system combining TGP and immortalized hepatocytes described in this study demonstrated efficient support of natural HCV infection and replication. This system may be used in future virological studies to define new anti-HCV strategies. It may also prove useful for the specific design of effective individual therapy according to patient-specific strains.

Acknowledgments

This work was supported by Grants-in-Aid from the Ministry of Health, Labor and Welfare of Japan; and for scientific research from Ministry of Education, Sports, Culture, and Technology of Japan.

References

[1] Z. Younossi, J. Kallman, J. Kincaid, The effects of HCV infection and management on health-related quality of life, Hepatology 45 (2007) 806–816.

[2] M.W. Fried, M.L. Shiffman, K.R. Reddy, C. Smith, G. Marinos, F.L. Goncales Jr., D. Haussinger, M. Diago, G. Carosi, D. Dhumeaux, A. Craxi, A. Lin, J. Hoffman, J. Yu, Peginterferon alfa-2a plus ribavirin for chronic hepatitis C virus infection, N. Engl. J. Med. 347 (2002) 975–982.
[3] K. Murakami, K. Ishii, Y. Ishihara, S. Yoshizaki, K. Tanaka, Y. Gotoh, H. Aizaki, M. Kohara, H. Yoshioka, Y. Mori, N. Manabe, I. Shoji, T. Sata, R. Bartenschlager, Y. Matsuura, T. Miyamura, T. Suzuki, Production of infectious hepatitis C virus particles in three-dimensional cultures of the cell line carrying the genome-length dicistronic viral RNA of genotype 1b, Virology 351 (2006) 381–392.
[4] G. Andrei, Three-dimensional culture models for human viral diseases and antiviral drug development, Antiviral Res. 71 (2006) 96–107.
[5] H.H. Aly, K. Watashi, M. Hijikata, H. Kaneko, Y. Takada, H. Egawa, S. Uemoto, K. Shimotohno, Serum-derived hepatitis C virus infectivity in interferon regulatory factor-7-suppressed human primary hepatocytes, J. Hepatol. 46 (2007) 26–36.
[6] K. Goto, K. Watashi, T. Murata, T. Hishiki, M. Hijikata, K. Shimotohno, Evaluation of the anti-hepatitis C virus effects of cyclophilin inhibitors, cyclosporin A and NIM811, Biochem. Biophys. Res. Commun. 343 (2006) 879–884.
[7] T. Murata, M. Hijikata, K. Shimotohno, Enhancement of internal ribosome entry site-mediated translation and replication of hepatitis C virus by PD98059, Virology 340 (2005) 105–115.
[8] M.A. El-Farrash, H.H. Aly, K. Watashi, M. Hijikata, H. Egawa, K. Shimotohno, In vitro infection of immortalized primary hepatocytes by HCV genotype 4a and inhibition of virus replication by cyclosporin, Microbiol. Immunol. 51 (2007) 127–133.
[9] J. Samulin, I. Berget, S. Lien, H. Sundvold, Differential gene expression of fatty acid binding proteins during porcine adipogenesis, Comp. Biochem. Physiol. B: Biochem. Mol. Biol. 151 (2008) 147–152.
[10] S. Hummasti, B.A. Laffitte, M.A. Watson, C. Galardi, L.C. Chao, L. Ramamurthy, J.T. Moore, P. Tontonoz, Liver X receptors are regulators of adipocyte gene expression but not differentiation: identification of apoD as a direct target, J. Lipid Res. 45 (2004) 616–625.
[11] C.G. Walker, M.J. Holness, G.F. Gibbons, M.C. Sugden, Fasting-induced increases in aquaporin 7 and adipose triglyceride lipase mRNA expression in adipose tissue are attenuated by peroxisome proliferator-activated receptor alpha deficiency, Int. J. Obes. (Lond.) 31 (2007) 1165–1171.
[12] D.G. Jump, D. Botolin, Y. Wang, J. Xu, B. Christian, O. Demeure, Fatty acid regulation of hepatic gene transcription, J. Nutr. 135 (2005) 2503–2506.
[13] D.W. Crabb, S. Liangpunsakul, Alcohol and lipid metabolism, J. Gastroenterol. Hepatol. 21 (Suppl. 3) (2006) 556–560.
[14] D. Panigrahy, A. Kaipainen, S. Huang, C.E. Butterfield, C.M. Barnes, M. Fannon, A.M. Laforme, D.M. Chaponis, J. Folkman, M.W. Kieran, PPARalpha agonist fenofibrate suppresses tumor growth through direct and indirect angiogenesis inhibition, Proc. Natl. Acad. Sci. USA 105 (2008) 985–990.
[15] V.S. Deshpande, J.P. Kehrer, Mechanisms of *N*-acetylcysteine-driven enhancement of MK886-induced apoptosis, Cell Biol. Toxicol. 22 (2006) 303–311.
[16] K.J. Blight, A.A. Kolykhalov, C.M. Rice, Efficient initiation of HCV RNA replication in cell culture, Science 290 (2000) 1972–1974.
[17] R.C. Dickson, Clinical manifestations of hepatitis C, Clin. Liver Dis. 1 (1997) 569–585.
[18] E.J. Heathcote, Antiviral therapy: chronic hepatitis C, J. Viral Hepat. 14 (Suppl. 1) (2007) 82–88.
[19] C.N. Palmer, M.H. Hsu, K.J. Griffin, J.L. Raucy, E.F. Johnson, Peroxisome proliferator activated receptor-alpha expression in human liver, Mol. Pharmacol. 53 (1998) 14–22.
[20] B. Rakic, S.M. Sagan, M. Noestheden, S. Belanger, X. Nan, C.L. Evans, X.S. Xie, J.P. Pezacki, Peroxisome proliferator-activated receptor alpha antagonism inhibits hepatitis C virus replication, Chem. Biol. 13 (2006) 23–30.

THE JOURNAL OF BIOLOGICAL CHEMISTRY VOL. 284, NO. 11, pp. 6841–6846, March 13, 2009

Heat-shock Protein 90 Is Essential for Stabilization of the Hepatitis C Virus Nonstructural Protein NS3*

Received for publication, August 20, 2008, and in revised form, December 22, 2008 Published, JBC Papers in Press, January 16, 2009, DOI 10.1074/jbc.M806452200

Saneyuki Ujino[‡], Saori Yamaguchi[‡], Kunitada Shimotohno[§¶], and Hiroshi Takaku[‡‖1]

From the [‡]Department of Life and Environmental Sciences, [‖]High Technology Research Center, and [§]Research Institute, Chiba Institute of Technology, 2-17-1 Tsudanuma, Narashino, Chiba 275-0016, Japan and the [¶]Center for Integrated Medical Research, School of Medicine, Keio University, Shinanomachi, Tokyo 160-8582, Japan

The hepatitis C virus (HCV) is a major cause of chronic liver disease. Here, we report a new and effective strategy for inhibiting HCV replication using 17-allylaminogeldanamycin (17-AAG), an inhibitor of heat-shock protein 90 (Hsp90). Hsp90 is a molecular chaperone with a key role in stabilizing the conformation of many oncogenic signaling proteins. We examined the inhibitory effects of 17-AAG on HCV replication in an HCV replicon cell culture system. In HCV replicon cells treated with 17-AAG, we found that HCV RNA replication was suppressed in a dose-dependent manner, and interestingly, the only HCV protein degraded in these cells was NS3 (nonstructural protein 3). Immunoprecipitation experiments showed that NS3 directly interacted with Hsp90, as did proteins expressed from ΔNS3 protease expression vectors. These results suggest that the suppression of HCV RNA replication is due to the destabilization of NS3 in disruption of the Hsp90 chaperone complex by 17-AAG.

Infection by the hepatitis C virus (HCV)[2] is a major public health problem, with 170 million chronically infected people worldwide (1, 2). The current treatment by combined interferon-ribavirin therapy fails to cure the infection in 30–50% of cases (3, 4), particularly those with HCV genotypes 1 and 2. Chronic infection with HCV results in liver cirrhosis and can lead to hepatocellular carcinoma (5, 6). Although an effective combined interferon-α-ribavirin therapy is available for about 50% of the patients with HCV, better therapies are needed, and preventative vaccines have not yet been developed.

HCV is a member of the *Flaviviridae* family and has a positive strand RNA genome (7, 8) that encodes a large precursor polyprotein, which is cleaved by host and viral proteases to generate at least 10 functional viral proteins: core, E1 (envelope 1), E2, p7, NS2 (nonstructural protein 2), NS3, NS4A, NS4B, NS5A, and NS5B (9, 10). NS2 and the amino terminus of NS3 comprise the NS2-3 protease responsible for cleavage between NS2 and NS3 (9, 11), whereas NS3 is a multifunctional protein consisting of an amino-terminal protease domain required for processing NS3 to NS5B (12, 13). NS4A is a cofactor that activates the NS3 protease function by forming a heterodimer (14–17), and the hydrophobic protein NS4B induces the formation of a cytoplasmic vesicular structure, designated the membranous web, which is likely to contain the replication complex of HCV (18, 19). NS5A is a phosphoprotein that appears to play an important role in viral replication (20–23), and NS5B is the RNA-dependent RNA polymerase of HCV (24, 25). The 3′-untranslated region consists of a short variable sequence, a poly(U)-poly(UC) tract, and a highly conserved X region and is critical for HCV RNA replication and HCV infection (26–29).

Hsp90 (heat-shock protein 90) is a molecular chaperone that plays a key role in the conformational maturation of many cellular proteins. Hsp90 normally functions in association with other co-chaperone proteins, which together play an important role in folding newly synthesized proteins and stabilizing and refolding denatured proteins in cells subjected to stress (30–34). Its expression is induced by cellular stress and is also associated with many types of tumor. Hsp90 inhibitors are currently showing great promise as novel pharmacological agents for anticancer therapy.

Hsp90 inhibitors have two major modes of action as preferential clients for protein degradation or as Hsp70 inducers. The benzoquinone ansamycin antibiotic geldanamycin and its less toxic analogue 17-allylamino-17-demethoxygeldanamycin (17-AAG) directly bind to the ATP/ADP binding pocket of Hsp90 (34–36) and thus prevent ATP binding and the completion of client protein refolding. Recently, Waxman *et al.* (37) demonstrated a role for Hsp90 in promoting the cleavage of HCV NS2/3 protease, using NS2/3 translated by rabbit reticulocyte lysate. Nakagawa *et al.* (38) also reported that inhibition of Hsp90 is highly effective in suppressing HCV genome replication. Hsp90 may directly or indirectly interact with any of the proteins NS3 through NS5B to regulate replication of the HCV replicon. More recently, Okamoto *et al.* (39) reported that Hsp90 could bind to FKBP8 (FK506-binding protein 8) and form a complex with NS5A. The interaction with FKBP8 has also been shown to be the mechanism by which Hsp90 regulates HCV RNA replication, a process in which Hsp90 clearly plays an important role.

In this study, we have demonstrated that NS3 also forms a complex with Hsp90, which is critical for HCV replication. On the basis of the findings that treating HCV replicon cells with

* This work was supported by a grant-in-aid for HCV research from the Ministry of Health, Labor, and Welfare of Japan and by a grant-in-aid for high technology research from the Ministry of Education, Science, Sports, and Culture of Japan. The costs of publication of this article were defrayed in part by the payment of page charges. This article must therefore be hereby marked "*advertisement*" in accordance with 18 U.S.C. Section 1734 solely to indicate this fact.

[1] To whom correspondence should be addressed: Dept. of Life and Environmental Science and High Technology Research Center, Chiba Institute of Technology, 2-17-1 Tsudanuma, Narashino-shi, Chiba 275-0016, Japan. Tel.: 81-47-478-0407; Fax: 81-47-471-8764; E-mail: hiroshi.takaku@it-chiba.ac.jp.

[2] The abbreviations used are: HCV, hepatitis C virus; 17-AAG, 17-allylamino-17-demethoxygeldanamycin.

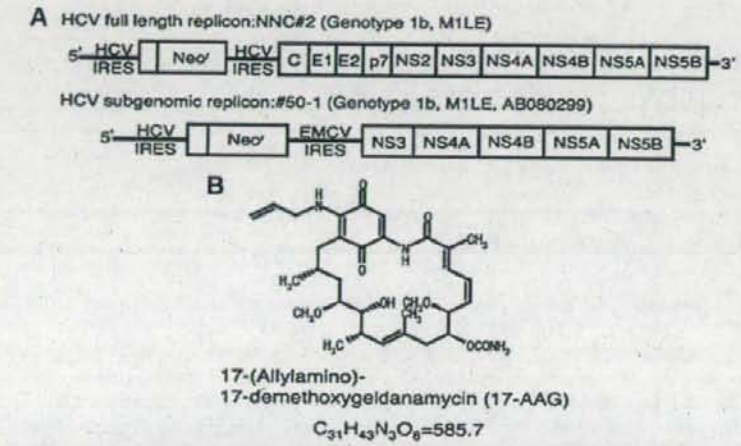

FIGURE 1. **Schematic representation of HCV replicon and structure of 17-AAG.** *A*, structure of the HCV replicon RNAs, comprising the HCV 5′-untranslated region, including the HCV internal ribosome entry site (*IRES*), the neomycin phosphotransferase gene (*Neo'*), the encephalomyocarditis virus (*EMCV*) IRES or HCV IRES, and the coding region for HCV proteins NS3 to NS5B (in the HCV subgenomic replicon) or core to NS5B (in the HCV full-length replicon). *B*, structures of the Hsp90 inhibitor, 17-AAG.

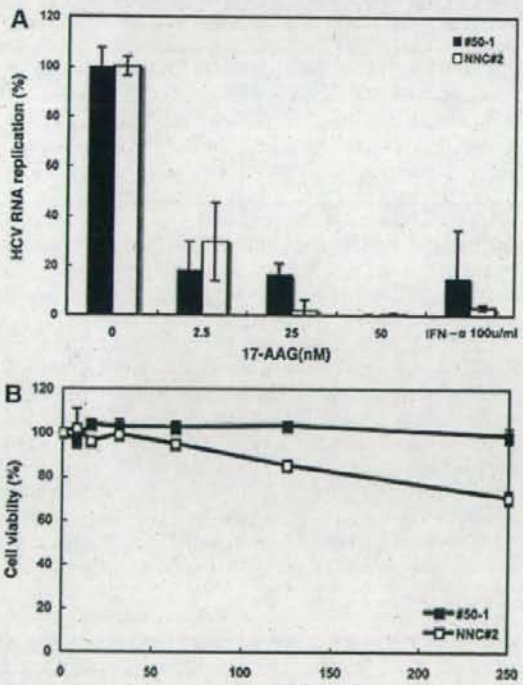

FIGURE 2. **Hsp90 inhibits HCV RNA replication in HCV replicon cells.** *A*, inhibition of HCV replication by 17-AAG in NNC#2 (*white squares*) and #50-1 cells (*black squares*) measured by real time reverse transcription-PCR after 72 h. Interferon-α was used as a positive control. The data are means ± S.D. from triplicate experiments. *B*, cytotoxic effects of 17-AAG in NNC#2 (*white squares*) and #50-1 (*black squares*), shown as the percentage reduction in viable cell numbers in an [3-(4,5-dimethylthiazol-2-yl)-5-(3-carboxymethoxyphenyl)-2-(4-sulfophenyl)-2H-tetrazolium (inner salt)] assay. The data are means ± S.D. from triplicate experiments.

the Hsp90 inhibitor, 17-AAG, suppressed HCV RNA replication, and that the only HCV protein degraded in these cells was NS3, we suggest a crucial role for Hsp90-NS3 protein complexes in the HCV life cycle.

EXPERIMENTAL PROCEDURES

Cell Culture and Reagents—The HCV replicon cell lines #50-1 (NN/1b/SG) (40), which carries a subgenomic replicon, and NNC#2 (NN/1b/FL) (41), which carries a full genome replicon, were cultured in Dulbecco's modified Eagle's medium supplemented with 10% fetal bovine serum, nonessential amino acids, L-glutamine, penicillin/streptomycin, and 300–1,000 μg/ml G418 (Invitrogen) at 37 °C in 5% CO_2. The human embryonic kidney-derived cell line 293T was grown in Dulbecco's modified Eagle's medium supplemented with 10% fetal bovine serum, 100 units/ml penicillin, and 100 μg/ml streptomycin. 17-AAG was purchased from Sigma.

Measuring HCV RNA by Real Time PCR—HCV replicon cells were seeded at 1.5×10^5 cells in 24-well plates and cultured for 72 h. Total RNA was then isolated using TRIzol (Invitrogen) according to the manufacturer's instructions. HCV RNA was quantified by real time reverse transcription-PCR using an ABI 7700 sequence detector (PerkinElmer Life Sciences) and the following primers and TaqMan probes located in the 5′-untranslated region: forward primer (nucleotides 130–146), 5′-CGGGAGAGCCATAGTGG-3′; reverse primer (nucleotides 272–290), 5′-AGTACCACAAGGCCTTTCG-3′; and TaqMan probe (nucleotides 148–168), 5′-CTGCGGAACCG-GTGAGTACAC-3′ (all purchased from Applied Biosystems). The probe sequence was labeled with the reporter dye, 6-carboxyflurorescein, at the 5′-end and with the quencher dye TAMRA at the 3′-end (42).

Western Blotting and Immunoprecipitation Analyses—Cells were lysed in 1× CAT enzyme-linked immunosorbent assay buffer (Roche Applied Sciences). Cell lysates were separated by SDS-PAGE and transferred to nitrocellulose membranes, and these were blocked with 5% skimmed milk. The primary antibodies used were monoclonal or polyclonal antibody against FLAG-M5 (Sigma), Hsp70 (Sigma), Hsp90 (Cell Signaling Technologies, Danvers, MA), Hsp90α (Calbiochem), Hsp90β (Calbiochem), and Hsf-1 (Calbiochem). Core, NS4A, and NS4B were a gift from Dr. M. Kohara (Tokyo Metropolitan Institute of Medical Science). E1, E2, NS3, NS5A, and NS5B were a gift from Prof. Y. Matsuura (Osaka University, Japan). Immunoprecipitation from cell lysates was carried out using anti-FLAG M5 antibody (Sigma) and the Protein G immunoprecipitation kit (Sigma), according to the manufacturer's instructions, and the immunoprecipitates were analyzed by Western blotting.

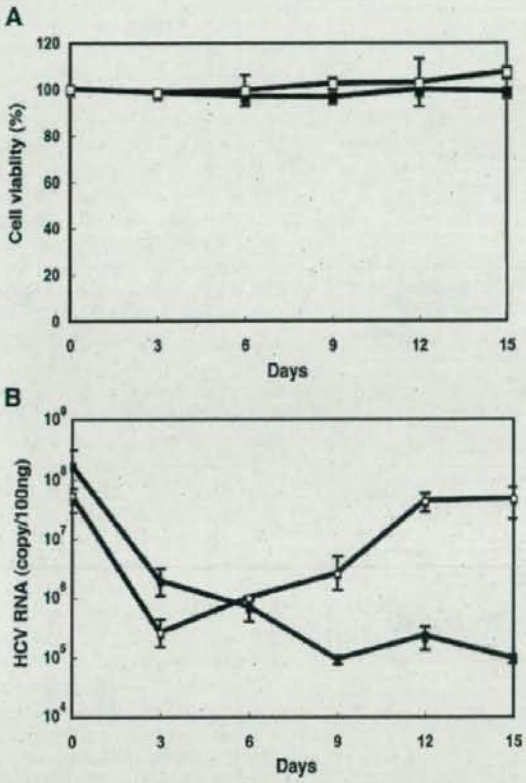

FIGURE 3. **Long term inhibition of HCV replication in NNC#2 cells.** *A*, cytotoxic effect of 17-AAG in NNC#2 cells, shown as the percentage reduction of viable cell numbers assessed by trypan blue staining. NNC#2 cells were treated with 50 nM 17-AAG on day 0 only (*white squares*) or at 3-day intervals for 15 days (*black squares*). The data are means ± S.D. from triplicate experiments. *B*, measurement of HCV replication by real time reverse transcription-PCR. Inhibition of HCV RNA replication in NNC#2 cells treated with 50 nM 17-AAG on day 0 only (*white squares*) or at 3-day intervals for 15 days (*black squares*). *Day 0*, mock. The data are means ± S.D. from triplicate experiments.

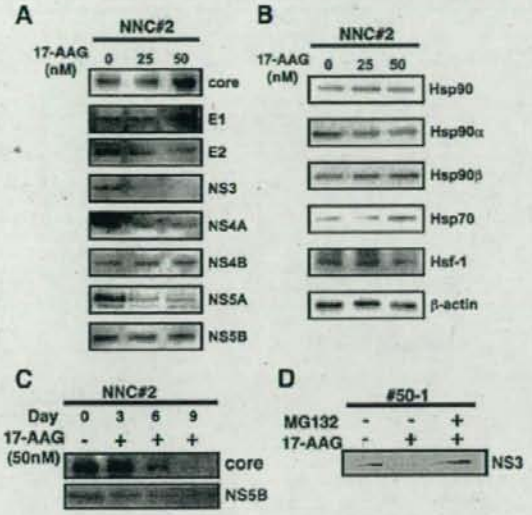

FIGURE 4. **Effect of 17-AAG on HCV NS3 protein levels.** *A*, Western blot analysis of HCV protein expression in NNC#2 or #50-1 cells treated with 17-AAG. NNC#2 or #50-1 cells were treated with 25 and 50 nM 17-AAG for 3 days. Cell lysates were separated by SDS-PAGE, immunoblotted, and probed with antibodies specific for HCV core, E1, E2, NS3, NS4A, NS4B, NS5A, and NS5B. *B*, Western blot analysis of Hsp90, Hsp70, and other chaperone expression in NNC#2 cells treated with 17-AAG (25 and 50 nM, as indicated) for 3 days. *C*, expression of HCV core and NS5B protein in cells treated with 50 nM 17-AAG for 9 days. *D*, effect of 50 nM 17-AAG on NS3 expression in #50-1 cells simultaneously treated with 100 nM MG132.

[3-(4,5-dimethylthiazol-2-yl)-5-(3-carboxymethoxyphenyl)-2-(4-sulfophenyl)-2H-tetrazolium, inner salt Assay—HCV replicon cells were seeded in 96-well plates at 3×10^4 cells/well in a final culture volume of 100 μl for 72 h before the addition of increasing concentrations of 17-AAG. After incubation for 3 days, viable cell numbers were determined using the Celltiter 96 Aqueous nonradioactive cell proliferation assay (Promega Corp., Madison, WI). The value of the background absorbance at 490 nm (A_{490}) of wells without cells was subtracted. The percentages of viable cells were then calculated using the formula, (A_{490} of 17-AAG-treated sample/A_{490} of untreated cells) × 100.

Plasmids and Transfection—The pFLAG-CMV-NS3 vector was constructed by subcloning a DNA fragment encoding full-length NS3, Δhelicase, Δprotease, ΔPH 1, ΔPH 2, and ΔH 1 into the EcoRI and XbaI sites of the pFLAG-CMV™-2 expression vector (Sigma), so that the amino-terminal FLAG epitope was fused in frame with NS3. The core expression vector was a gift from Dr. M. Kohara. The vector was transfected into 293T cells using the FuGENE 6 transfection reagent (Roche Applied Science) according to the manufacturer's instructions.

RESULTS

Hsp90 Inhibitor 17-AAG Suppresses HCV RNA Replication—To investigate the effect of 17-AAG on HCV replication, cells containing a full HCV genome replicon (NNC#2) or a subgenomic replicon (#50-1) were treated with 17-AAG (Fig. 1, *A* and *B*). Both of the HCV replicon cell lines were treated for 72 h with different concentrations of 17-AAG or with DMSO as a control. In cells treated with 50 nM 17-AAG, HCV RNA replication was suppressed by 99% in both of the HCV replicon cell lines, and the inhibition of RNA replication occurred in a dose-dependent manner (Fig. 2*A*). The half-maximal inhibitory concentration (IC_{50}) values of 17-AAG for HCV replication were 0.3 nM in NNC#2 cells and 0.1 nM in #50-1 cells. Furthermore, we used a tetrazolium-based [3-(4,5-dimethylthiazol-2-yl)-5-(3-carboxymethoxyphenyl)-2-(4-sulfophenyl)-2H-tetrazolium, inner salt assay to determine the viability of NNC#2 and #50-1 cells in the presence of 17-AAG. 17-AAG showed no toxicity to NNC#2 and #50-1 cells at 50 nM, (Fig. 2*B*). These results suggested that 17-AAG had a greater inhibitory effect on HCV RNA replication than 100 units/ml interferon-α.

Long Term Suppression of HCV RNA Replication—We next examined the effect of 17-AAG on HCV replication over time. When NNC#2 cells were cultured with 50 nM 17-AAG only on day 0 (*white squares*), the level of HCV RNA was reduced by 2 log on day 3 but had increased to control levels by day 12 (Fig.

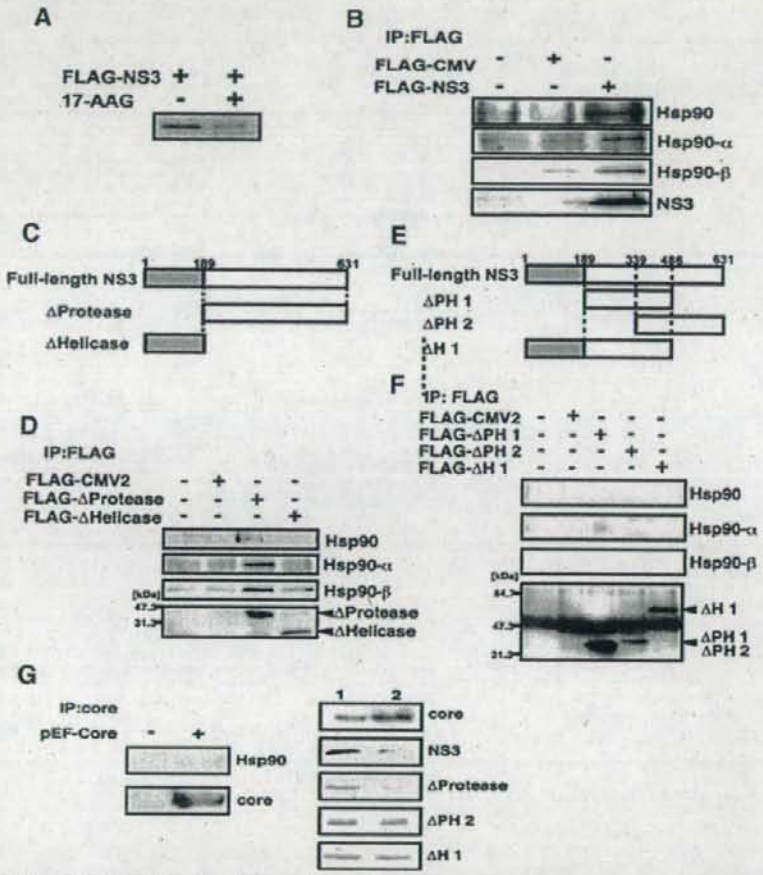

FIGURE 5. **Hsp90 regulates HCV NS3 protein stability.** *A*, Western blot showing the inhibition of NS3 protein expression in 293T cells caused by 17-AAG. Cells were transfected with pFLAG-NS3 in the presence of 250 nM 17-AAG for 48 h. *B*, FLAG-NS3 was expressed in 293T cells and immunoprecipitated (*IP*) from cell lysates with anti-FLAG antibody. Proteins immunoprecipitated were analyzed by Western blotting using anti-Hsp90, anti-Hsp90α, anti-Hsp90β, and anti-FLAG antibodies. The data shown in each *panel* are representative of three independent experiments. *FLAG-CMV*, empty plasmid vector. *C*, schematic representations of HCV NS3 protein and its deletion mutants. *D*, FLAG-NS3, FLAG-Δprotease, and FLAG-Δhelicase were expressed in 293T cells and immunoprecipitated from cell lysates with anti-FLAG antibody. Proteins immunoprecipitated with anti-Hsp90, Hsp90α, Hsp90β, and FLAG antibodies were analyzed by Western blotting. The data shown in each panel are representative of three independent experiments. *E*, schematic representations of HCV NS3 protein and further deletion mutants. *F*, FLAG-ΔPH 1, FLAG-ΔPH 2, and FLAG-ΔH 1 were expressed in 293T cells and immunoprecipitated from cell lysates with anti-FLAG antibody. Proteins immunoprecipitated with anti-Hsp90, Hsp90α, Hsp90β, and FLAG antibodies were analyzed by Western blotting. The data shown in each panel are representative of three independent experiments. *G*, FLAG-NS3, pEF-Core, FLAG-Δprotease, FLAG-ΔPH 2, and FLAG-ΔH 1 were expressed in 293T cells treated with 17-AAG. Proteins immunoprecipitated with anti-core, Hsp90 antibody were analyzed by Western blotting. 17-AAG-treated cell lysates were analyzed on Western blots, using the specific antibodies shown to the *right* of the panels. *Lane 1*, control; *lane 2*, 17-AAG (1 μM).

3*B*). However, when 50 nM 17-AAG was added to the cells at 3-day intervals for 15 days (*black squares*), the observed significant reduction in HCV RNA (by 3 log) was sustained from day 3 to day 15. We used trypan blue staining to check that long term treatment with 17-AAG did not induce cellular toxicity (Fig. 3*A*). Our results suggested that 17-AAG has the potential to safely induce long term suppression in HCV replication.

Reduced Expression of NS3 Protein in 17-AAG-treated HCV Replicon Cells—To investigate the mechanism by which 17-AAG inhibited HCV replication, we analyzed the expression of HCV core, E1, E2, NS3, NS4A, NS4B, NS5A, and NS5B proteins by Western blotting. NNC#2 cells treated with increasing doses of 17-AAG showed a marked reduction in the expression of NS3 (Fig. 4*A*) after 3 days, in common with the level of HCV RNA (Fig. 2*A*). However, levels of the other proteins were unchanged. This dose-dependent inhibition suggested that NS3 was more sensitive to 17-AAG than the other proteins. Similar effects on NS3 expression and RNA replication were seen in #50-1 cells treated with 17-AAG (Fig. 4*A*).

Another effect of 17-AAG treatment seen in these cells was an increase in Hsp70 expression and a slight increase in Hsp90 expression (Fig. 4*B*). The induction of Hsp70 expression suggested that Hsp90 inhibition by 17-AAG strongly activated HSF-1 (heat-shock transcription factor 1) (43). We also examined the levels of HCV core and NS5B protein expression in NNC#2 cells treated with 50 nM 17-AAG. Reduced levels of these proteins were seen in NNC#2 cells on day 6, and both HCV core and NS5B protein were undetectable on day 9 (Fig. 4*C*). To determine whether 17-AAG promoted the degradation of NS3, we next looked at the effect of 17-AAG on #50-1 cells in which proteasomal degradation was also inhibited. Although 17-AAG treatment still induced a reduction in the NS3 protein level in #50-1 cells (Fig. 4*D*), the degradation of NS3 was completely blocked in the presence of the proteasome inhibitor, MG132. This suggested that the pharmacological effect of 17-AAG was dependent on the proteasome system (44, 45).

Protein Folding in Hsp90-NS3 Interaction—To investigate the role of Hsp90 in HCV NS3 activation, the FLAG-NS3 protein was transfected into 293T cells, with or without 17-AAG, and the cell lysates were analyzed by Western blotting. The expression of NS3 from FLAG-NS3 was reduced in the presence of 17-AAG (Fig. 5*A*), suggesting that Hsp90 is involved in HCV NS3 degradation, possibly through a physical interaction.

We confirmed this specific interaction by immunoprecipitating 293T cell lysates with anti-FLAG antibody. This clearly showed that FLAG and Hsp90 co-precipitated, suggesting that NS3 was bound to the chaperone complex formed with Hsp90 (Fig. 5*B*). NS3 mutants lacking the protease and helicase regions were generated in order to identify the region responsible for the interaction with Hsp90 (Fig. 5*C*). FLAG-NS3, FLAG-NS3-Δhelicase, or FLAG-NS3-Δprotease were transfected into 293T cells, and anti-FLAG antibody immunoprecipitates were analyzed by Western blotting (Fig. 5*D*). Although FLAG-NS3-Δprotease was clearly co-immunoprecipitated with Hsp90, no protein band corresponding to FLAG-NS3-Δhelicase was detected (Fig. 5*D*), suggesting that the NS3 helicase region mediates binding to Hsp90. To confirm this finding, plasmids expressing different NS3 helicase mutants fused with FLAG (ΔPH 1, ΔPH 2, and ΔH 1) were constructed (Fig. 5*E*). Expressing these NS3 helicase mutants in 293T cells and analyzing their immunoprecipitates with anti-FLAG antibody by Western blotting showed that, although all of the NS3 helicase mutant proteins were immunoprecipitated by anti-FLAG-antibody, no Hsp90 was co-precipitated (Fig. 5*F*).

We also confirmed that the NS3 helicase region mediated the specific interaction with Hsp90 by transfecting FLAG-NS3 and FLAG-NS3 deletion mutants into 293T cells pretreated with 17-AAG (Fig. 5*G*). The proteins expressed by FLAG-NS3 and FLAG-NS3-Δprotease were degraded in cells pretreated with 17-AAG, whereas no degradation of the ΔPH 2 and ΔH 1 NS3 mutants lacking helicase regions was seen (Fig. 5*G*). Further, when pEF-core was expressed in 293T cells, core was unable to co-immunoprecipitate Hsp90, and no degradation of core protein was observed (Fig. 5*G*). Our data demonstrate that 17-AGG destabilizes several binding proteins (NS3 and NS3-Δprotease) to Hsp90 but stablilizes some nonbinding proteins (the ΔPH 2 and ΔH 1 NS3 mutants lacking helicase regions and core) to Hsp90. In previous reports (46), similar effects were observed when wild-type and mutated p53 were translated in the presence of geldanamycin. These results further supported the hypothesis that Hsp90 has a role in folding the NS3 helicase domain and that this has an important role in stabilizing the full-length NS3 protein. A protein complex that includes NS3 and Hsp90 is therefore implicated in the control of HCV replication.

DISCUSSION

The Hsp90 inhibitor, 17-AAG, is known to have highly selective effects on tumor cells that are a result of its high affinity for Hsp90 client oncoproteins, which are incorporated into the Hsp90-dependent multichaperone complex, thereby increasing their binding affinity for 17-AAG more than 100-fold (47). This high selectivity effectively minimizes the toxic side effects of 17-AAG so that it is a good candidate for clinical application, especially in treating neurodegenerative diseases. In this study, we observed the inhibitory effects of 17-AAG on the replication of an HCV subgenomic replicon that lacked NS2. On the other hand, Waxman *et al.* (37) demonstrated a role for Hsp90 in promoting the cleavage of HCV NS2/3 protein using NS2/3 translated in rabbit reticulocyte lysate and expressed in Jurkat cells. Because the replicon cells used in our study genetically lacked NS2, our results suggest that Hsp90 may directly interact with the NS3 protein in the HCV replicon.

In cell lines in which 17-AAG was a potent inhibitor of HCV replication, with IC_{50} values of 3–10 nM, we also found strong evidence that the association between HCV Hsp90 and NS3, but not other NS proteins, was the essential mechanism controlling the preferential degradation of NS3 after 17-AAG treatments. Furthermore, we showed that NS3 interacted with Hsp90 through the NS3 helicase domain. It was also clear that the expression of NS3 protein with helicase activity in 293T cells pretreated with 17-AAG was reduced, but the expression of NS3 mutants lacking the helicase regions (ΔPH 2 and ΔH 1) was not. The role of Hsp90 in achieving and/or stabilizing the NS3 protein was suggested by the fact that only 17-AGG bound to Hsp90 was capable of affecting NS3. The use of Hsp90 inhibitors represents a novel strategy for the development of anti-HCV therapies.

Acknowledgments—We are grateful to M. Sato, R. Tobita, and Y. Katumura for excellent technical assistance.

REFERENCES

1. Alter, H. J., Purcell, R. H., Shih, J. W., Melpolder, J. C., Houghton, M., Choo, Q. L., and Kuo, G. (1989) *N. Engl. J. Med.* **321,** 1494–1500
2. Choo, Q. L., Kuo, G., Weiner, A. J, Overby, L. R., Bradley, D. W., and Houghton, M. (1989) *Science* **244,** 359–362
3. McHutchison, J. G., Gordon, S. C., Schiff, E. R., Shiffman, M. L., Lee, W. M., Rustgi, V. K., Goodman, Z. D., Ling, M. H., Cort. S., and Albrecht, J. K. (1998) *N. Engl. J. Med.* **339,** 1485–1492
4. Glue, P., Rouzier-Panis, R., Raffanel, C., Sabo, R., Gupta, S. K., Salfi, M., Jacobs, S., and Clement, R. P. (2000) *Hepatology* **32,** 647–653
5. Saito, I., Miyamura, T., Ohbayashi, A., Harada, H., Katayama, T., Kikuchi, S., Watanabe, Y., Koi, S., Onji, M., and Ohtaet, Y. (1990) *Proc. Natl. Acad. Sci. U. S. A.* **87,** 6547–6549
6. Seeff, L. B. (1997) *Hepatology* **26,** 21S–28S
7. Bartenschlager, R., and Lohmann, V. (2001) *Antiviral Res.* **52,** 1–17
8. Taylor, D. R., Shi, S. T., Romano, P. R., Barber, G. N., and Lai, M. M. (1999) *Science* **285,** 107–110
9. Grakoui, A., Wychowski, C., Lin. C., Feinstone, S. M., and Rice, C. M. (1993) *J. Virol.* **67,** 1385–1395
10. Hijikata, M., Mizushima, H., Akagi, T., Mori, S., Kakiuchi, N., Kato, N., Tanaka, T., Kimura, K., and Shimotohno, K. (1993) *J. Virol.* **67,** 4665–4675
11. Grakoui, A., McCourt, D. W., Wychowski, C., Feinstone, S. M., and Rice, C. M. (1993) *Proc. Natl. Acad. Sci. U. S. A.* **90,** 10583–10587
12. Bartenschlager, R., Ahlborn-Laake, L., Mous, J., and Jacobsen, H. (1993) *J. Virol.* **67,** 3835–3844
13. Grakoui, A., McCourt, D. W., Wychowski, C., Feinstone, S. M., and Rice, C. M. (1993) *J. Virol.* **67,** 2832–2843
14. Bartenschlager, R., Lohmann, V., Wilkinson, T., and Koch, J. O. (1995) *J. Virol.* **69,** 7519–7528
15. Failla, C., Tomei, L., and De Francesco, F. (1995) *J. Virol.* **69,** 1769–1777
16. Lin, C., Thomson, J. A., and Rice, C. M. (1995) *J. Virol.* **69,** 4373–4380
17. Tanji, Y., Hijikata, M., Satoh, S., Kaneko, T., and Shimotohno, K. (1995) *J. Virol.* **69,** 1575–1581
18. Egger, D., Wolk, B., Gosert, R., Bianchi, L., Blum, H. E., Moradpour, D., and Bienz, K. (2002) *J. Virol.* **76,** 5974–5984
19. Gosert, R., Egger, D., Lohmann, V., Bartenschlager, R., Blum, H. E., Bienz, K., and Moradpour, D. (2003) *J. Virol.* **77,** 5487–5492
20. Blight, K. J., Kolykhalov, A. A., and Rice, C. M. (2000) *Science* **290,** 1972–1974
21. Guo, J. T., Bichko, V. V., and Seeger, C. (2001) *J. Virol.* **75,** 8516–8523
22. Krieger, N., Lohmann, V., and Bartenschlager, R. (2001) *J. Virol.* **75,** 4614–4624

23. Lohmann, V., Hoffmann, S., Herian, U., Penin, F., and Bartenschlager, R. (2003) *J. Virol.* **77,** 3007–3019
24. Behrens, S. E., Tomei, L., and De Francesco, R. (1996) *EMBO J.* **15,** 12–22
25. Lohmann, V., Korner, F., Herian, U., and Bartenschlager, R. (1997) *J. Virol.* **71,** 8416–8428
26. Friebe, P., and Bartenschlager, R. (2002) *J. Virol.* **76,** 5326–5338
27. Kolykhalov, A. A., Mihalik, K., Feinstone, S. M., and Rice, C. M. (2000) *J. Virol.* **74,** 2046–2051
28. Yanagi, M., St. Claire, M., Emerson, S. U., and Purcell Bukh, J. (1999) *Proc. Natl. Acad. Sci. U. S. A.* **96,** 2291–2295
29. Yi, M., and Lemon, S. M. (2003) *J. Virol.* **77,** 3557–3568
30. Picard, D. (2002) *Cell Mol. Life Sci.* **59,** 1640–1648
31. Wegele, H., Muller, L., and Buchner, J. (2004) *Rev. Physiol. Biochem. Pharmacol.* **151,** 1–44
32. Pratt, W. B., and Toft, D. O. (2003) *Exp. Biol. Med.* **228,** 111–133
33. Smith, D. F., Whitesell, L., and Katsanis, E. (1998) *Pharmacol. Rev.* **50,** 493–514
34. McClellan, A. J., and Frydaman, J (2001) *Nat. Cell Biol.* **3,** E1–E3
35. Grenert, J. P., Sullivan, W. P., Fadden, P., Haystead, T. A., Clark, J., Mimnaugh, E., Krutzsch, H., Ochel, H. J., Schulte, T. W., Sausville, E., Neckers, L. M., and Toft, D. O. (1997) *J. Biol. Chem.* **272,** 23843–23850
36. Supko, J. G., Hickman, R. L., Grever, M. R., and Malspeis, L. (1995) *Cancer Chemother. Pharmacol.* **36,** 305–315
37. Waxman, L., Whitney, M., Pollok, B. A., Kuo, L. C., and Darke, P. L. (2001) *Proc. Natl. Acad. Sci. U. S. A.* **98,** 13931–13935
38. Nakagawa, S., Umehara, T., Matsuda, C., Kuge, S., Sudoh, M., and Kohara, M. (2007) *Biochem. Biophys. Res. Commun.* **353,** 882–888
39. Okamoto, T., Nishimura, Y., Ichimura, T., Suzuki, K., Miyamura, T., Suzuki, T., Moriishi, K., and Matsuura, Y. (2006) *EMBO J.* **25,** 5015–5025
40. Kishine, H., Sugiyama, K., Hijikata, M., Kato, N., Takahashi, H., Noshi, T., Nio, Y., Hosaka, M., Miyanari, Y., and Shimotohno, K. (2002) *Biochem. Biophys. Res. Commun.* **290,** 993–999
41. Ishii, N., Watashi, K., Hishiki, T., Goto, K., Inoue, D., Hijikata, M., Wakita, T., Kato, N., and Shimotohno, K. (2006) *J. Virol.* **80,** 4510–4520
42. Takeuchi, T., Katsume, A., Tanaka, T., Abe, A., Inoue, K., Tsukiyama-kohara, K., Kawaguchi, R., Tanaka, S., and Kohara, M. (1999) *Gastroenterology* **11,** 636–642
43. Sittler, A., Lurz, R., Ueder, G., Priller, J., Lehrach, H., Hayer-Hartl, M. K., Hartl, F. U., and Wanker, E. E. (2001) *Hum. Mol. Genet.* **10,** 1307–1315
44. Bonvini, P., Dalla Rosa, H., Vignes, N., and Rosolen, A. (2004) *Cancer Res.* **64,** 3256–3264
45. Mimnaugh, E. G., Chavany, C., and Neckers, L. (1996) *J. Biol. Chem.* **271,** 22796–22801
46. Blagosklonny, M. V., Toretsky, J., Bohen, S., and Neckers L. (1996) *Proc. Natl. Acad. Sci. U. S. A.* **93,** 8379–8383
47. Kamal, A., Thao, L., Sensintaffar, J., Zhang, L., Boehm, M. F., Fritz, L. C., and Burrows, F. J. (2003) *Nature* **425,** 357–359

Bioorganic & Medicinal Chemistry Letters 18 (2008) 4638–4641

Contents lists available at ScienceDirect

Bioorganic & Medicinal Chemistry Letters

journal homepage: www.elsevier.com/locate/bmcl

Synthesis and evaluation of 5′-modified 2′-deoxyadenosine analogues as anti-hepatitis C virus agents

Masahiro Ikejiri [a,b,*], Takayuki Ohshima [a], Akemi Fukushima [a], Kunitada Shimotohno [c], Tokumi Maruyama [a,*]

[a] Faculty of Pharmaceutical Sciences at Kagawa Campus, Tokushima Bunri University, 1314-1 Shida, Sanuki, Kagawa 769-2193, Japan
[b] Faculty of Pharmacy, Osaka Ohtani University, 3-11-1 Nishikiori-kita, Tondabayashi, Osaka 584-8540, Japan
[c] Center for Integrated Medical Research, Keio University School of Medicine, 35 Shinanomachi, Shinjuku, Tokyo 160-8582, Japan

ARTICLE INFO

Article history:
Received 9 June 2008
Revised 3 July 2008
Accepted 5 July 2008
Available online 10 July 2008

Keywords:
Antiviral agent
Hepatitis C virus
HCV
Nucleoside

ABSTRACT

In order to study the effect of 5′-modification of 2′-deoxynucleoside on its anti-HCV activity, several analogues were synthesized and evaluated. Among the analogues, a 5′-deoxy-5′-phenacylated analogue exhibited a good anti-HCV activity with an EC_{50} of 15.1 μM. This compound is expected to operate via a type of mechanism that does not involve a generally known 5′-*O*-triphosphorylation process.

Hepatitis C virus (HCV)[1] is a major causative agent of non-A and non-B hepatitis. It is estimated to have infected >170 million individuals, that is, 3.5% of the world's population. HCV infection is a leading cause of chronic hepatitis, liver cirrhosis and hepatocellular carcinoma. Current therapy based on pegylated interferon and ribavirin is often poorly tolerated and is effective in only 50% of patients. Therefore, the development of further effective therapeutic agents against HCV is an urgent public health requirement.

In our previous study,[2] we revealed that several 5′-*O*-masked analogues of 6-chloropurine-2′-deoxyriboside, such as benzoate **1** and benzyl ether **2**, exhibit an effective anti-HCV activity in a subgenomic replicon cell line and are more potent than the corresponding unmasked analogue **3** (Fig. 1). Since it is generally accepted that most nucleoside antivirals exhibit their potency after being converted to the corresponding 5′-triphosphates,[3] the unmasked (or phosphorylated) 5′-hydroxyl group is indispensable for the antiviral activity. Accordingly, our result that the 5′-*O*-masking leads to an improvement in the anti-HCV activity appears to be inconsistent with the common understanding, interestingly.

We presume that the anti-HCV activity of certain 5′-*O*-masked analogues would arise from a new type of mechanism that does not involve the 5′-*O*-triphosphorylation process. However, there is still room for the discussion on the 5′-*O*-masking effect because certain carbon–oxygen bonds, for example, the carboxylic ester bond of compound **1** (i.e., the benzoate moiety in compound **1**), are often hydrolyzed in cultured cells; in other words, there is a possibility that compound **1** simply operates as a prodrug of **3**.[4,5] Therefore, in order to confirm the effectiveness of 5′-*O*-masking groups, particularly that of the benzoyl group of compound **1**, we planned the syntheses and anti-HCV evaluations of ketone analogues **4** and **5**, in which the 5′-oxgen atom was replaced with a methylene group to prevent the hydrolytic removal of the benzoyl group.

The synthesis of **4** began with readily available 3′-*O*-TBS-2′-deoxyadenosine (**6**)[6] (Scheme 1). First, we attempted to subject

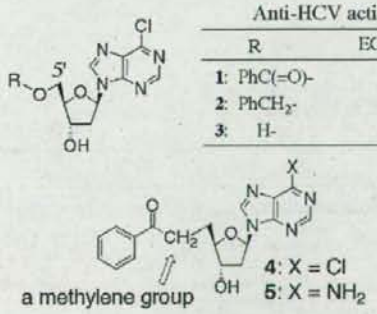

Anti-HCV activity

R	EC_{50} (μM)
1: PhC(=O)-	6.1
2: $PhCH_2$-	17.7
3: H-	47.2

Figure 1. Structures of 5′-modified analogues.

* Corresponding authors.
E-mail address: ikejim@osaka-ohtani.ac.jp (M. Ikejiri).

0960-894X/$ - see front matter © 2008 Elsevier Ltd. All rights reserved.
doi:10.1016/j.bmcl.2008.07.015

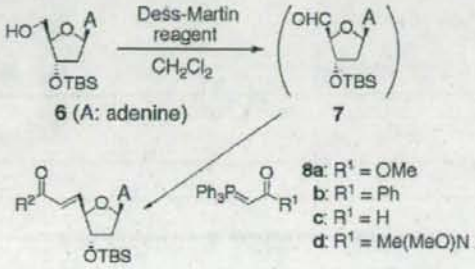

compd	R^2	yield (%)	*E*:*Z*
9	MeO–	90	*E* only
10	Ph–	60	13:1
11	H–	—	
12	Me(MeO)N–	—	

Scheme 1.

the isolated aldehyde **7** obtained via the oxidation of **6** to the following Wittig reaction; however, it was unsuccessful due to the instability of **7**. This issue was overcome by using a one-pot oxidation–Wittig reaction with Dess–Martin periodinane (DMP) and stabilized phosphorus ylide.[7] Among the four types of ylides examined (**8a–d**), two of them (**8a** and **8b**) successfully afforded the desired compounds **9** and **10** in 90% (*E*-isomer only) and 60% (*E*:*Z* = 13:1) yields, respectively, while the others (**8c** and **8d**) yielded complex mixtures. Since the Dess–Martin oxidation is not very suitable for the large-scale synthesis of **9** and **10** because of the explosive nature of DMP (and also its precursor, 2-iodoxybenzoic acid[8]), several other one-pot protocols such as Moffatt oxidation–Wittig,[9] PCC–Wittig,[10] TEMPO–BAIB–Wittig,[11] and TPAP–NMO–Wittig[12] were examined with **6** and **8a**. However, the TLC analyses of all the attempts revealed low yields and/or the formation of by-products.

With the thus-obtained products, the reduction of the C–C double bond was examined (Table 1). Compound **9** was converted to **13** under standard hydrogenation conditions (Pd/C, H_2, THF) with an excellent yield although the reaction required a long reaction time (~2 days) and comparatively large quantities of the catalyst (50 wt.%) (entry 1). In contrast, the conjugate reduction of **9** by sodium borohydride–transition metal salt (e.g., $NiCl_2$ and CuCl) systems[13] furnished **13** in a short time (1–3 h), but the yield was moderate (entries 2 and 3). The use of elemental magnesium in methanol led to a complex mixture (entry 4). In the case of **10**, chemoselective hydrogenations by Sajiki's procedures (Pd/fibroin–H_2 or Pd/C–Ph_2S–H_2)[14] were ineffective, resulting in the recovery of a large amount of the starting material (entries 5 and 6), while the 1,4-reduction with indium hydride generated in situ by using $PhSiH_3$–$In(OAc)_3$ or Bu_3SnH–$InCl_3$[15] efficiently afforded the desired product **14** in good yields (entries 7 and 8). Consequently, the conditions in the case of entries 1 and 7 were employed for routine syntheses of **13** and **14**, respectively, in view of their simple experimental procedures as well as their good yields.

Table 1
Chemoselective reduction of C–C double bond

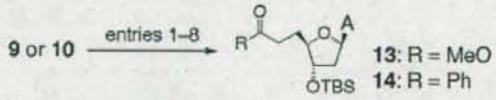

Entry	Substrate	Conditions	Product	Yield (%)
1	**9**	Pd/C, H_2, THF, rt, 2 d	**13**	94
2	**9**	$NiCl_2$, $NaBH_4$, MeOH, 0 °C, 1 h	**13**	50
3	**9**	CuCl, $NaBH_4$, MeOH, 0 °C, 2.5 h	**13**	76
4	**9**	Mg, MeOH, reflux, 2 h	Complex mix.	
5	**10**	Pd/fibroin, H_2, MeOH, rt, 2 d	**14**	Trace[a]
6	**10**	Pd/C, Ph_2S, H_2, MeOH, rt, 2 d	**14**	31[b]
7	**10**	$PhSiH_3$, $In(OAc)_3$, EtOH, rt, over night	**14**	84
8	**10**	Bu_3SnH, $InCl_3$, *i*-PrOH −78 °C to rt, 2 h	**14**	93

[a] 93% of **10** was recovered.
[b] 56% of **10** was recovered.

Compound **13** was readily converted to **14** with a two-step sequence, that is, via a Weinreb amide **15**, as illustrated in Scheme 2-A. Using a Grignard reagent (PhMgBr) led to a better yield (71%) than when phenyl lithium was used (58% yield). This two-step conversion will effectively serve for the synthesis of various analogues because the phenyl moiety of **14** can be easily replaced with other groups by changing the type of Grignard reagent. The amino group of **14** was substituted by a chloro group to afford **16** (40% yield),

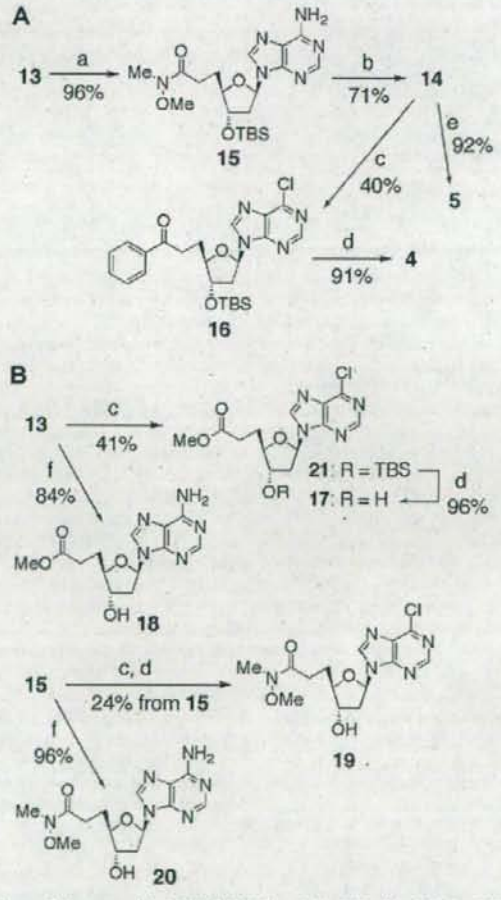

Scheme 2. Reagents: (a) Me(MeO)NH·HCl, *n*-BuLi, THF; (b) PhMgBr, THF; (c) *t*-BuONO, Et_4NCl, CCl_4–CH_2Cl_2; (d) TBAF, AcOH, THF; (e) Et_3N·3HF, THF; (f) TAS-F, MeCN.

which was subsequently treated with a mixture of tetrabutylammonium fluoride (TBAF) and acetic acid, giving the desired product **4** in 91% yield. A moderate yield of **16** was mainly obtained due to the competitive elimination of its nucleobase moiety. The other desired compound **5** was prepared in 92% yield by exposing **14** to triethylamine trihydrofluoride.

Since we are interested in the structure–activity relationship (SAR) of not only the benzoyl moiety but also the methyl ester and Weinreb amide moieties contained in the synthetic intermediates, we conducted syntheses of the corresponding analogues **17–20**, as shown in Scheme 2-B. 6-Chloropurine analogues **17** and **19** were prepared from **13** and **15**, respectively, under conditions almost identical to those used in the synthesis of **4** (i.e., *t*-BuONO–Et_4NCl and TBAF–AcOH). The conversion to **18** and **20** was effectively accomplished by the treatment of **13** and **15** with tris(dimethylamino)sulfonium difluorotrimethylsilicate (TAS-F),[16] while that with TBAF led to a mixture of the desired product and certain tertabutylammonium salts that were difficult to separate.

The synthesized nucleoside analogues mentioned above were assayed for their ability to inhibit HCV RNA replication in a subgenomic replicon Huh7 cell line (LucNeo#2),[17] and the result is presented in Table 2 and Figure 2. These cells contain an HCV subgenomic replicon RNA encoding a luciferase reporter gene as a marker. The antiviral potency of the analogues against the HCV replicon is expressed as EC_{50}, which was quantified by a luciferase assay after a two-day incubation period with the corresponding compound. In addition, the associated cytotoxicity (expressed as CC_{50} in Table 2) was evaluated in a tetrazolium (XTT)-based assay according to the manufacturer's protocol.

As shown in Table 2, the ketone analogue **4** exhibited an antiviral activity against the HCV replicon with an EC_{50} of 15.1 μM (entry 1), which is nearly comparable to that of benzoate analogue **1** (entry 7). The cytotoxicity of **4** was somewhat high (CC_{50}: 76.3 μM), but was not high enough to exert an influence on the EC_{50} value because the cytotoxicity at 15 μM was considerably low (ca. 0–2%) (Fig. 2A). Thus, the decrease in the luciferase activity with **4** results from its anti-HCV activity, not its cytotoxicity. Interestingly, compounds **17** and **19** also exhibited anti-HCV activities (entries 3 and 5, respectively). In contrast, the 6-amino analogues **5**, **18**, and **20** did not exhibit any significant anti-HCV activity (entries 2, 4, and 6).[18]

To confirm the anti-HCV potency of compound **4**, subgenomic replicon RNA levels were quantified by real-time RT-PCR analysis (Fig. 2B). Exposing the replicon cells to 12.5 and 25 μM of **4** reduced the replicon RNA amount up to approximately 60% and 25%, respectively. This result is almost consistent with that of the luciferase assay with **4**.

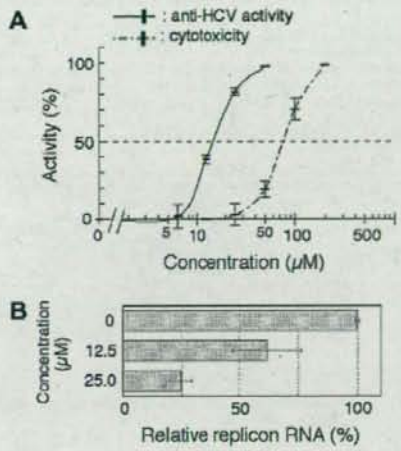

Figure 2. Anti-HCV activity and cytotoxicity of **4**: (A) result of luciferase assay and XTT assay; (B) result of real-time RT-PCR.

Taking these data into account, it appears that the phenacyl group ($BzCH_2$–) equipped at the C5′ position as well as the benzoyloxy group (BzO–) is effective functional group for anti-HCV activity; this should be noteworthy because the 5′-phenacyl group is expected to operate without being converted to the corresponding 5′-hydroxyl group (or 5′-triphosphate group). This result strongly supports our hypothesis that the 5′-*O*-masking group can contribute to the anti-HCV activity not only as a unit for the prodrug system but also as a part of the substrate. Although the detailed mechanism is unclear and the biological activity is still insufficient, the antiviral potency of such 5′-modified analogues is of great interest because they are likely to operate via a pathway that does not involve the 5′-*O*-phosphorylation process. We hope that the present study will contribute to developing a new class of HCV therapeutic agents.

Table 2
Inhibitory potency (EC_{50}) and cytotoxicity (CC_{50}) of the synthesized analogues in HCV replicon assay

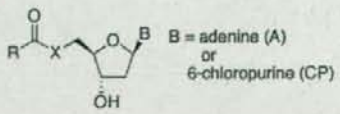

Entry	Compound	R	X	B	EC_{50}[a] (μM)	CC_{50}[a] (μM)
1	**4**	Ph	CH_2	CP	15.1 ± 0.4	76.3 ± 5.2
2	**5**	Ph	CH_2	A	>200	–
3	**17**	MeO	CH_2	CP	32.9 ± 1.6	>200
4	**18**	MeO	CH_2	A	>200	–
5	**19**	Me(MeO)N	CH_2	CP	40.4 ± 1.4	>200
6	**20**	Me(MeO)N	CH_2	A	>200	–
7	**1**	Ph	O	CP	6.1[b]	111[b]

[a] EC_{50}: 50% effective concentration; CC_{50}: 50% cytotoxic concentration.
[b] Extracts obtained from our previous study (Ref. 2).

Acknowledgments

This research was partly supported by a Grant-in-Aid for Young Scientists (B) (20790106) from the Ministry of Education, Culture, Sports, Science and Technology of Japan and by a Grant-in-Aid from Mitsubishi Chemical Corporation Fund.

Supplementary data

Supplementary data associated with this article (experimental details and spectroscopic data of new compounds **4–6**, **9**, **10**, **13–21**) can be found, in the online version, at doi:10.1016/j.bmcl.2008.07.015.

References

1. Recent reviews: (a) Gordon, C. P.; Keller, P. A. *J. Med. Chem.* **2005**, *48*, 1; (b) De Francesco, R.; Migliaccio, G. *Nature* **2005**, *436*, 953; (c) De Clercq, E. *Nat. Rev. Drug Discov.* **2007**, *6*, 1001.
2. Ikejiri, M.; Ohshima, T.; Kato, K.; Toyama, M.; Murata, T.; Shimotohno, K.; Maruyama, T. *Bioorg. Med. Chem.* **2007**, *15*, 6882.
3. Arimilli, M. N.; Dougherty, J. P.; Cundy, K. C.; Bischofberger, N.. In *Advances in Antiviral Drug Design*; De Clercq, E., Ed.; Jai Press Inc.: Stamford Connecticut, 1999; Vol. 3, pp 69–91. and also see Refs. 1a and c and references therein.

4. Several 5′-O-acyl nucleoside analogues have been reported as prodrugs of the corresponding deacylated analogues Parang, K.; Wiebe, L. I.; Knaus, E. E. *Curr. Med. Chem.* **2000**, *7*, 995.
5. Not only compound **1** but also **2** might operate as a prodrug of **3** since O-dealkylated metabolism is caused in some cases. Silverman, R. B. *The Organic Chemistry of Drug Design and Drug Action, Second Edition*; Elsevier, 2004, Chapter 7.
6. Somu, R. V.; Wilson, D. J.; Bennett, E. M.; Boshoff, H. I.; Celia, L.; Beck, B. J.; Barry, C. E., III; Aldrich, C. C. *J. Med. Chem.* **2006**, *49*, 7623.
7. Barrett, A. G. M.; Hamprecht, D.; Ohkubo, M. *J. Org. Chem.* **1997**, *62*, 9376.
8. A one-pot oxidation–Wittig reaction with 2-iodoxybenzoic acid is also reported Crich, D.; Mo, X.-S. *Synlett* **1999**, 67.
9. Rapp, M.; Haubrich, T. A.; Perrault, J.; Mackey, Z. B.; McKerrow, J. H.; Chiang, P. K.; Wnuk, S. F. *J. Med. Chem.* **2006**, *49*, 2096.
10. Bressette, A. R.; Glover, L. C., IV *Synlett* **2004**, 738.
11. Vatèle, J.-M. *Tetrahedron Lett.* **2006**, *47*, 715.
12. MacCoss, R. N.; Balskus, E. P.; Ley, S. V. *Tetrahedron Lett.* **2003**, *44*, 7779.
13. (a) Narisada, M.; Horibe, I.; Watanabe, F.; Takeda, K. *J. Org. Chem.* **1989**, *54*, 5308; (b) Satoh, T.; Nanba, K.; Suzuki, S. *Chem. Pharm. Bull.* **1971**, *19*, 817.
14. (a) Ikawa, T.; Sajiki, H.; Hirota, K. *Tetrahedron* **2005**, *61*, 2217; (b) Mori, A.; Mizusaki, T.; Miyakawa, Y.; Ohashi, E.; Haga, T.; Maegawa, T.; Monguchi, Y.; Sajiki, H. *Tetrahedron* **2006**, *62*, 11925.
15. (a) Miura, K.; Yamada, Y.; Tomita, M.; Hosomi, A. *Synlett* **2004**, 1985; (b) Inoue, K.; Ishida, T.; Shibata, I.; Baba, A. *Adv. Synth. Catal.* **2002**, *344*, 283.
16. Kang, S. B.; De Clercq, E.; Lakshman, M. K. *J. Org. Chem.* **2007**, *72*, 5724.
17. (a) Watashi, K.; Hijikata, M.; Hosaka, M.; Yamaji, M.; Shimotohno, K. *Hepatology* **2003**, *38*, 1282; (b) Murata, T.; Hijikata, M.; Shimotohno, K. *Virology* **2005**, *340*, 105; (c) Goto, K.; Watashi, K.; Murata, T.; Hishiki, T.; Hijikata, M.; Shimotohno, K. *Biochem. Biophys. Res. Commun.* **2006**, *343*, 879. And also see Ref. 2.
18. A similar SAR trend was observed in our previous study. Ikejiri, M.; Saijo, M.; Morikawa, S.; Fukushi, S.; Mizutani, T.; Kurane, I.; Maruyama, T. *Bioorg. Med. Chem. Lett.* **2007**, *17*, 2470.